IN-SITU GENERATION OF POLY(N-VINYL-2-PYRROLIDONE)-STABILIZED PALLADIUM(0) AND RUTHENIUM(0) NANOCLUSTERS AS CATALYSTS FOR HYDROGEN GENERATION FROM THE METHANOLYSIS OF AMMONIA-BORANE

A THESIS SUBMITTED TO
THE GRADUATE SCHOOL OF NATURAL AND APPLIED SCIENCES
OF
MIDDLE EAST TECHNICAL UNIVERSITY

BY

HURİYE ERDOĞAN

IN PARTIAL FULFILLMENT OF THE REQUIREMENT
FOR
THE DEGREE OF MASTER OF SCIENCE
IN
CHEMISTRY

MAY 2010

Approval of the thesis:

IN-SITU GENERATION OF POLY(N-VINYL-2-PYRROLIDONE)-STABILIZED PALLADIUM(0) AND RUTHENIUM(0) NANOCLUSTERS AS CATALYSTS FOR HYDROGEN GENERATION FROM THE METHANOLYSIS OF AMMONIA-BORANE

Submitted by **HURİYE ERDOĞAN** in partial fulfillment of the requirements for the degree of **Master of Science in Department of Chemistry, Middle East Technical University** by,

Prof. Dr. Canan ÖZGEN
Dean, Graduate School of **Natural and Applied Sciences**

Prof. Dr. İlker ÖZKAN
Head of Department, **Chemistry**

Prof. Dr. Saim ÖZKAR
Supervisor, **Chemistry Dept., METU**

Examining Committee Members:

Prof. Dr. Ceyhan KAYRAN
Chemistry Dept., METU

Prof. Dr. Saim ÖZKAR
Chemistry Dept., METU

Prof. Dr. İnci EROĞLU
Chemical Engineering Dept., METU

Prof. Dr. Yavuz İMAMOĞLU
Chemistry Dept., Hacettepe University

Assoc. Prof. Dr. Ayşen YILMAZ
Chemistry Dept., METU

Date: 25.05.2010

I hereby declare that all information in this document has been obtained and presented in accordance with academic rules and ethical conduct. I also declare that, as required by these rules and conduct, I have fully cited and referenced all material and results that are not original to this work.

Name, Last name : Huriye ERDOĞAN

Signature :

ABSTRACT

IN-SITU GENERATION OF POLY(N-VINYL-2-PYRROLIDONE)-STABILIZED PALLADIUM(0) AND RUTHENIUM(0) NANOCLUSTERS AS CATALYSTS FOR HYDROGEN GENERATION FROM THE METHANOLYSIS OF AMMONIA-BORANE

Erdoğan, Huriye
M.Sc., Department of Chemistry
Supervisor: Prof. Dr. Saim ÖZKAR

May 2010, 83 pages

More attention has been paid to find new type renewable energy sources because of increasing concern about the environmental problems arising from the combustion of fossil fuels as energy sources. The development of new storage materials will facilitate the use of hydrogen as a major energy carrier. Several possibilities exist for ‘‘solid-state’’ storage: the hydrogen can be trapped in metal organic frameworks, carbon nanotubes and certain alloys; or one can use materials in which hydrogen is already present in the composition (e.g., chemical hydrides). The latter option seems to be the most promising since it permits a higher mass ratio of hydrogen. Recently, ammonia-borane complex (NH_3BH_3, AB) has been considered as solid hydrogen storage material since it possess one of the highest hydrogen contents (19.6 wt. %) and high stability under the moderate conditions. Hydrolysis and methanolysis are the two reactions liberating hydrogen from AB. However, a catalyst is needed for hydrogen generation from methanolysis of AB. In this context, we aim to develop PVP-stabilized palladium(0) and ruthenium(0) nanoclusters as catalyst for the methanolysis of AB.

The PVP-stabilized palladium(0) and ruthenium(0) nanoclusters were prepared from the in-situ reduction of palladium(II) acetylacetonate and ruthenium(III) chloride respectively in the methanolysis of AB. The prepared palladium(0) nanoclusters were isolated as solid materials by removing the volatile in vacuum and characterized by using TEM, SAED, XPS, FT-IR, XRD and UV-visible electronic absorption spectroscopy techniques while and ruthenium(0) nanoclusters were characterized by TEM, XPS, XRD, FT-IR and UV-visible electronic absorption spectroscopy techniques. The kinetics of methanolysis of AB catalyzed by palladium(0) and ruthenium(0) nanoclusters were studied depending on the catalyst concentration, substrate concentration and temperature. The activation parameters of the catalytic methanolysis reaction obtained from the evaluation of kinetic data.

Keywords: Nanoclusters, Catalyst, Methanolysis of Ammonia Borane, PVP, Hydrogen, Palladium, Ruthenium.

ÖZ

AMONYAK BORANIN METANOLİZİNDEN HİDROJEN ÜRETİMİNİ KATALİZLEYEN POLİ(N-VİNiL-2-PİROLİDON) İLE KARARLILAŞTIRILMIŞ VE REAKSİYON ANINDA SENTEZLENMİŞ PALADYUM(0) VE RUTENYUM(0) NANOKÜMELERİ

Erdoğan, Huriye
Yüksek Lisans, Kimya Bölümü
Tez Yöneticisi: Prof. Dr. Saim ÖZKAR

Mayıs 2010, 83 sayfa

Fosil yakıtların kullanımından kaynaklı çevresel kirliliği önlemek amacıyla yenilenebilir enerji kaynaklarına yönelim artmaktadır. Yeni depolama malzemelerinin bulunmasıyla hidrojen enerjisi de gelecekte yenilenebilir enerji kaynakları arasında önemli bir konuma sahip olacaktır. Hidrojeni katı halde depolamak için birçok yöntem bulunmaktadır. Hidrojenin depolanması, metal organik sistemlere (karbon nanotüpler, alaşımlar) konularak ya da yapısında zaten hidrojen bulunduran kimyasal hidrürlerin kullanılmasıyla mümkündür. Yapılarında kütlece yüksek yüzdelerde hidrojen bulunduran kimyasal hidrürlerin hidrojen depolama malzemesi olarak kullanımı daha avantajlıdır. Son zamanlarda amonyak-boran bileşiği (NH_3BH_3, AB) kütlece %19.6 hidrojen içermesi ve ortam koşullarındaki dayanıklılığı sebebiyle hidrojen depolama maddesi olarak oldukça ilgi çekmektedirler. AB'nin hidrolizi ve metanolizi sonucu hidrojen üretimi gerçekleşmektedir. AB'nin metanolizi sonucu hidrojen eldesi için uygun bir katalizöre gereksinim vardır.

Bu bağlamda, bu çalışmada poli(vinilpirolidon) ile kararlılaştırılmış paladyum(0) ve rutenyum(0) nanokümelerinin AB'nin metanolizinden hidrojen üretimi için katalizör olarak kullanılması amaçlanmıştır. Paladyum(0) ve rutenyum(0) nanokümeleri, paladyum(II) asetilasetonatın ve rutenyum(III) klorürün AB'nin metanolizi tepkimesinde eş zamanlı indirgenmesi ve PVP ile kararlılaştırılması yolu ile elde edildi. Hazırlanan nanokümelerinin uçucu kısımları vakum ile uzaklaştırıldı. Kalan katı paladyum(0) nanokümelerinin tanımlanması TEM, XPS, SAED, FT-IR, XRD ve UV-görünür elektronik absorpsiyon yöntemleri kullanılarak, rutenyum(0) nanokümelerinin tanımlanması ise TEM, XPS, XRD, FT-IR ve UV-görünür elektronik absorpsiyon yöntemleri ile yapıldı. Paladyum(0) ve rutenyum(0) nanokümeleri ile katalizlenen AB'nin metanolizinin kinetiği değişik katalizör derişimi, substrat derişimi ve sıcaklıklarda incelendi. Tepkimenin aktivasyon parametreleri kinetik verilere bağlı olarak değerlendirildi.

Anahtar Kelimeler: Nanokümeler, Katalizör, Amonyak Boranın Metanolizi, PVP, Hidrojen, Paladyum, Rutenyum.

Dedicated To My Family.

ACKNOWLEDGEMENTS

I would like to express my greatest appreciations to my supervisor Prof. Dr. Saim Özkar, for his encouragement, guidance and valuable advices.

I gratefully thank to Önder Metin for his support, valuable ideas and motivation during my studies.

I want to give special thanks to Osman Candaş Dağdaş for his endless valuable moral support.

I owe great thanks to my lab mates Tuğçe Ayvalı, Melek Dinç, Serdar Akbayrak, Mehdi Masjedi and Ebru Unel for their moral support, help and valuable discussions.

I would like to express my special thanks to my best friends Nagehan Keskin, Merve Bekarlar and especially to MSc. Sevinç Tunçağıl for their precious friendship.

I am thankful to my cousins and my home mates Tolga Erdoğan and Mehmet Erdoğan for making the time enjoyable and livable.

I would like to thank to Özge Toker and Müge Toker for their help and support.

I also would like to express my endless thanks to my parents Hasan Erdoğan, Selma Erdoğan and especially my brother Çağrı Erdoğan who made everything possible for me and who always being there whenever I need.

TABLE OF CONTENTS

LIST OF TABLES

TABLES

LIST OF FIGURES

FIGURES

CHAPTER 1

INTRODUCTION

Between the 20th and 21st centuries it was concluded that there was an urgent requirement for an alternative and sustainable energy source since reserves of fossil fuels died out [1]. Moreover, because the harmful effects of fossil fuels affecting climate change thus accelerated global warming creates a demand for green and renewable energy sources such as wind energy, solar energy, hydropower and biomass energy [2]. Since these resources' power plants constructions are costly and inefficient, hydrogen appeared to be an alternative way of obtaining clean energy. Hydrogen is not a primary energy source but is an energy carrier and it is globally accepted clean fuel which could overcome the world energy problem and reduce the environmental pollution caused by usage of fossil fuels as a primary energy source [3]. The main challenge for the widespread application of hydrogen is its real-time production and its safe and convenient storage. H_2 has low density which makes it difficult to store in compressed or liquid form [4]. Metal hydrides [5], metal organic frameworks [6], chemical hydrides [7] and hydrocarbons [8] have been tested as solid hydrogen storage materials hitherto. Although sodium borohydride has also been considered as solid hydrogen storage material [9], its use has been restricted to portable fuel cell applications because of its instability in solution without a base [10] and inefficacy in recycling the hydrolysis product [11] (Eq.1).

$$NaBH_4 + 2H_2O \xrightarrow{\text{catalyst}} NaBO_2 + 4H_2 \quad (1)$$

Recently, ammonia-borane (AB) has attracted much attention due to its high hydrogen capacity (19.6 wt. %), high stability and non-toxicity [12]. Hydrogen can be generated from AB via thermal decomposition [13], acid-catalyzed [14] or transition-metal catalyzed dehydrogenation [15,16,17] and hydrolysis [18].

In contrast to $NaBH_4$, ammonia-borane does not undergo self hydrolysis in water and only generates hydrogen through the hydrolysis reaction in the presence of suitable catalyst (Eq.2) [19].

$$H_3NBH_3 + 2H_2O \xrightarrow{\text{catalyst}} (NH_4)BO_2 + 3H_2 \quad (2)$$

Recent studies have shown that zeolite framework stabilized rhodium(0) nanoclusters and poly(N-vinyl-2-pyrrolidone)(PVP)-stabilized cobalt(0) nanoclusters are highly active catalysts for hydrogen generation from the hydrolysis of ammonia-borane [20]. However, liberation of small quantities of ammonia at high AB concentrations and inefficacy in recycling the hydrolysis product metaborate can pose problems for hydrogen generation from hydrolysis of AB in fuel cell applications. In this regard, methanolysis appears to be advantageous for hydrogen generation from AB (Eq.3) [21,22], as the methanolysis product can be regenerated and no ammonia is liberated in the methanolysis, two important requirements for fuel cell applications [12].

$$H_3NBH_3 + 4CH_3OH \xrightarrow{\text{catalyst}} NH_4B(OCH_3)_4 + 3H_2 \qquad (3)$$

Methanolysis of AB occurs only in the presence of a suitable catalyst. Herein, we report the employment of the in-situ generated, polymer–stabilized palladium(0) nanoclusters and ruthenium(0) nanoclusters as catalyst in the methanolysis of AB.

So far, Ramachandran and Gagare have tested various transition-metal salts such as $RuCl_3$, $RhCl_3$, $PdCl_2$ and $CoCl_2$ in the methanolysis of AB and shown that $RuCl_3$ is the catalyst of choice [12]. Although $RuCl_3$ provides high activity for the methanolysis of AB the report is lacking of information on the lifetime of the catalyst. As in the other two papers [21,22] it has not been reported for how long such a high TOF value would be retained. Also the issue whether the catalysis starting with the transition metal salts is homogeneous or heterogeneous has not been addressed [12]. It is noteworthy that the catalytic activity of two Pd catalysts, $PdCl_2$ and carbon-supported Pd, are very low [12]. Similarly, Pd supported on γ-Al_2O_3 has been reported to have much lower activity in the hydrolysis of AB compared to the other transition metals such Ru, Rh and Pt supported on γ-Al_2O_3 [23]. Despite the low catalytic activity of palladium in both the hydrolysis and methanolysis of AB, we have shown that the PVP-stabilized palladium(0) nanoclusters are highly active and long lived heterogeneous catalyst in the methanolysis of AB. Ruthenium is the one of the active metal catalyst even in the salt form [12,23]. But it is an expensive metal and need to be used in low amount without any loss. Although it is an active catalyst in the methanolysis of AB, its catalytic lifetime is unknown. In this thesis we have also shown that in-situ generated PVP-stabilized ruthenium(0) nanoclusters have an extraordinary catalytic activity in the methanolysis of AB.

The activity of the catalyst is depended on the surface area. Owing to the large surface area of the heterogeneous transition-metal nanoclusters catalysts, they exhibit large catalytic activity with respect to their bulk counterparts [24]. However they must be protected against agglomeration because transition-metal nanoclusters are thermodynamically unstable since they have higher surface free energy with respect to their lattice energy resulted from the large surface area compared to their masses.

Stabilization of metal nanoparticles can be achieved mainly in two ways: *(i)* electrostatic stabilization and *(ii)* steric stabilization [25].

Electrostatic stabilization is based on the complementary repulsion of like electrical charges. Anions and cations forms an electrical double layer and it intereacts with metallic particle surface [26]. In steric stabilization method, large organic molecules having long chains covered the surface of the nanoparticle by extending out their long loops and chains [27]. In this study, palladium(0) and ruthenium(0) nanoclusters were synthesized in-situ and stabilized by PVP which is a steric stabilization agent, for the first time.

The PVP-stabilized palladium(0) nanoparticles have been prepared via alcohol [28], polyol [29], microwave assisted [30] and chemical reduction method [31]. Similarly, PVP-stabilized ruthenium(0) nanoparticles have been synthesized by polyol [32], solvothermal method [33] and chemical reduction method [34] hitherto. For the catalytic applications, PVP-stabilized nanoparticles prepared by using one of these methods must be separated from the synthesis solution and redispersed in the solvent of catalysis. The separation processes generally result in a significant loss of catalyst. In this regard, the in situ generation of nanoparticles in the medium of catalytic reaction is important. Polymer-stabilized palladium(0) nanoclusters and ruthenium(0) nanoclusters were generated for the first time in-situ by the reduction of palladium(II) acetylacetonate and ruthenium(III) chloride respectively in the presence of poly(N-vinyl-2-pyrrolidone) PVP, during the methanolysis of AB. PVP-stabilized palladium(0) and ruthenium(0) nanoclusters are highly active catalyst in the methanolysis of AB and stable in solution. PVP-stabilized palladium(0) nanoclusters were isolated from the solution and characterized by TEM, XPS, FT-IR, XRD, SAED and UV-Visible electronic absorption spectroscopy. On the other hand, PVP-stabilized ruthenium(0) nanoclusters were characterized by TEM, XPS, XRD, FT-IR and UV-visible spectroscopy. The ability of Hg(0) to poison heterogeneous metal(0) catalysts [35], by amalgamating the metal catalyst or being adsorbed on its surface, has been known for a long time.

In order to identify whether our metal(0) nanoclusters are true heterogeneous catalyst in the methanolysis of AB or not, mercury poisoning test was used.

The detailed kinetics of the catalytic methanolysis of AB was also studied by measuring the volume of hydrogen generated during the reaction varying the catalyst concentration, substrate concentration and temperature. In addition to these, lifetimes of the catalysts were also investigated in the methanolysis of AB reaction.

CHAPTER 2

HYDROGEN ECONOMY

2.1. World Energy Problem

The century we are living in can be defined as a century where big energy consumptions and rapid increase in population worldwide occur with improving new technologies and increasing manmade materials. With the revolution of transport by invention of cars, new world has started to depend increasingly on combustion of hydrocarbon fuels such as gasoline, diesel fuel and jet fuel. Moreover, the invention of electrical power plants, household electrical appliances, personal computers and mobile cell phones have forced the world to use electricity generated largely from carbon-based resources such as coal and natural gas [36] .

A major challenge the world faced with is the fact that fossil resources are being depleted so fast. The resources of petroleum and natural gas that took tens of millions of years to form and accumulate have been consumed so rapid in the last 80 years that they have diminished to one to two human lifetimes [37].

Coinage of high-pressure ammonia synthesis and evolvement of the chemical fertilizers with nitrogen, phosphorus, potassium and the engine-based machinery for crop production accelerated the rapid growth in global population. Pollutants such as NOx, SOx and particulate matter and more importantly greenhouse gases (GHG) such as carbon dioxide (CO_2) and methane (CH_4) are emitted from combustion of solid, liquid and gaseous fuels in various stationary and mobile energy systems result in environmental problems thus lead to global warming [38]. These results attracted the world interest for minimizing the emissions of GHG, particularly CO_2 [39]. World must eliminate environmental pollution problems and find sustainable and safe energy sources namely renewable energy sources.

2.2. Hydrogen as a Solution of the Present Energy Problems

Hydrogen is the lightest most abundant element in the universe comprising about 75 % of the Universe's elemental mass. Although it's abundance, hydrogen does not exist as its pure form. It can be found in the form of chemical compounds such as hydrocarbons and water and need to be extracted. In 1493, T. Von Hohenheim produced hydrogen gas firstly by mixing strong acids with metals but in 1766, Henry Cavendish is the one who was the first to recognize hydrogen gas as a substance and isolated it. The element achieved its name as hydrogen (from the Greek *hydro* meaning water and *genes* meaning creator), in 1783 by Antoine Lavoisier [40,41].

As an energy carrier, hydrogen is considered to be a future solution of the current energy problems because it is nontoxic and its combustion does not create any pollution or greenhouse gases. Moreover, hydrogen is high in energy and does not need to be combusted; by electrochemical conversion method it is easy to provide useful energy from hydrogen. Besides these, it can be produced from all and any energy sources, including fossil fuels, nuclear energy and renewable energy sources. That is, it could be used as fuel in nearly all places where fossil fuels are used with offering direct benefits in terms of reduced pollution and cleaner environment [42].

Although hydrogen is served as an ideal energy carrier, there are still some challenges about production, storage and transportation of hydrogen. Since it is not found as its pure form, an extraction process is needed [43].

There are several methods are being used to produce hydrogen: *(i)* production of hydrogen by water electrolysis [44], *(ii)* direct thermal decomposition of water [45], *(iii)* thermochemical cycles [46], *(iv)* photolysis [47] and *(v)* hydrogen production from biomass [48].

Transportation of hydrogen is another issue that hydrogen economy faced with. Hydrogen should be transmitted to consumers in terms of underground pipelines (gaseous hydrogen) and/or supertankers (liquid hydrogen) [49].

The last struggle with hydrogen is its storage. Hydrogen is the lightest element (H_2 density is 0.03, 0.06 and 0.07 kg/L at 350 atm, 700 atm and liquefied (20 K), respectively [50]) so it is a struggle to store hydrogen in compressed or liquid form. Depending on the storage and size application, there are mainly four groups are merging under the title of hydrogen storage techniques: *(i)* compressed gas, *(ii)* cryogenic liquid, *(iii)* metal hydrides, and *(iv)* chemical hydrides [51].

2.3. Ammonia-Borane as a Hydrogen Storage Material

Hydrogen has been considered as a clean fuel that overcomes the world energy problem [52]. One difficulty occurring in hydrogen based energy economy is that, there should be a hydrogen storage material possessing high volumetric and gravimetric hydrogen storage density [53]. Hydrogen is the lightest element with a density: $0.08988 gL^{-1}$, this makes hydrogen too difficult to store in the gas form [54]. Chemical hydrides are served to be as an efficient hydrogen storage material and have been tested for supplying hydrogen under mild conditions.

Recently ammonia-borane (AB, H_3NBH_3) complex is used as a leading hydrogen storage material owing to its high hydrogen content (19.6 wt %), (Figure 1), low molecular weight (30.9 g/mol), non toxicity and stability in fuel cell reactions [55].

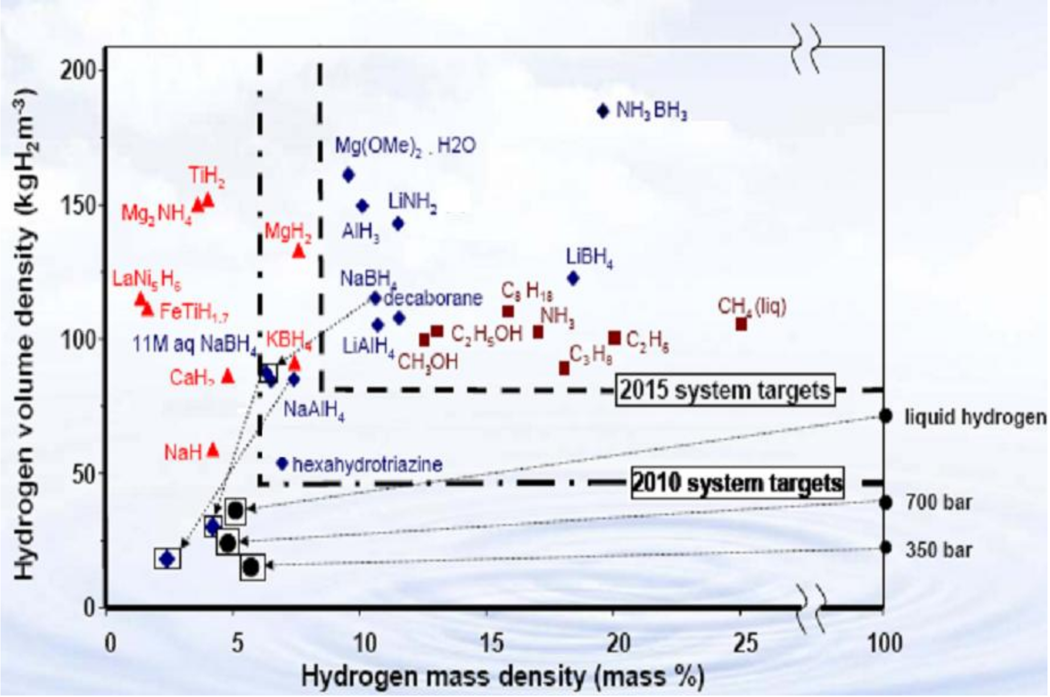

Figure 1. Volumetric hydrogen density versus gravimetric hydrogen density of various hydrogen containing compounds (adopted from the literature [56]).

AB composed of B and N atoms which creates a big electronegativity difference and contains both hydridic B–H and protonic N–H bonds within the same molecule. This fact results in strong molecular attractions between atoms, so AB is solid at room temperature which enables extra stability to AB at ambient temperatures. Moreover it is nontoxic and environmentally benign. AB can be easily handled and transported safely. The reactions of AB resulting hydrogen evolution are thermolysis [57], hydrolysis [58] and methanolysis [59,60].

A catalyst is vital to have a practical application for effective hydrogen production from AB. The catalyst that will be used must be economic and should change the rate and effectiveness of the reaction significantly. Other properties that must be improved for effective use of AB in fuel cell applications are that the reactions which generate hydrogen must be recyclable and the reaction should not evaluate ammonia (NH_3) gas.

These circumstances were achieved firstly by Ramachandran and co-workers who used an alcohol, methanol, instead of water. They achieved the recycling product of methanolysis (ammonium tetramethoxyborate) to ammonia-borane with high yields (81 %) and purity (98%) [12] (Eq. 3).

As stated above, methanolysis of AB seems to be advantageous over hydrolysis. Firstly, in the hydrolysis reaction, at higher concentration of substrate, that is AB, liberation of NH_3 gas is observed which considered as a problem in fuel cell applications. Secondly, the regeneration of the hydrolysis product to AB is difficult. These two problems can be handled over by methanolysis (Figure 2).

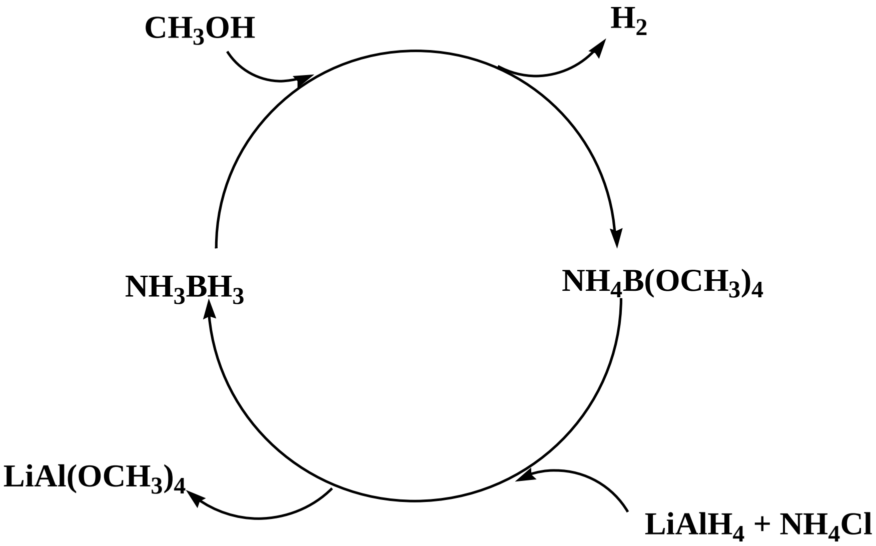

Figure 2. Ammonia-borane hydrogen cycle (taken from literature [12]).

However, methanolysis reaction cannot occur without a suitable catalyst [59]. Hitherto, various transition metal salts such as $RuCl_3$, $RhCl_3$, $PdCl_2$, $CoCl_2$, nano particles [21] like Cu NPs, Cu_2O, and nanocomposites [22] like Cu–Cu_2O, Co–Co_2B, Ni–Ni_3B, Co–Ni–B have been tested in the methanolysis of AB.

Although it can be understood from these reports that catalyst size has a remarkable effect on the methanolysis of AB, these studies lack of kinetic and catalytic lifetime studies information.

CHAPTER 3

TRANSITION METAL(0) NANOCLUSTERS AS CATALYST

3.1. General Principles of Catalysis

‘Alien’ materials are known to be the materials that are not included in the stochiometric equation of a reaction. A catalyst is an alien material that increases the rate of a chemical reaction without being consumed. This process is defined as catalysis when a catalyst acts.

Catalysts are classified as in three groups: *homogenous, heterogeneous* and *biological catalysts*. A *homogenous* catalyst defined as when the catalyst and the substrate are in the same medium that is to say there is not a phase boundary in the reaction. Organometallic complex catalysts mainly considered as homogenous type. Homogeneous catalysts are known to be more selective and live in relatively mild conditions than their heterogeneous counterparts. A *heterogeneous* type catalyst is in different phase with the substrate. Most of the time the catalyst is in the solid phase where the substrate is in liquid or gas phase. Since there is always a phase difference, isolation of the catalyst from the reaction medium is effortless. The usage of heterogeneous catalysts seems to have more advantages compare to homogenous type in terms of being stable, easy to handle, synthesize, and recycle. Moreover they are known to having low cost and low toxicity. This type is more abundant in industrial processes.

Enzymes are the *biological catalysts* composed of large, complex organic molecules usually contain proteins. They are essential for life, as they catalyze mainly all biological processes. A catalyst increases the rate of the reaction by decreasing the activation energy both forward and backward shown in Figure 3. As shown in the schematic representation, the activation energy needed for an uncatalyzed reaction is greater than the reaction when catalyzed is used.

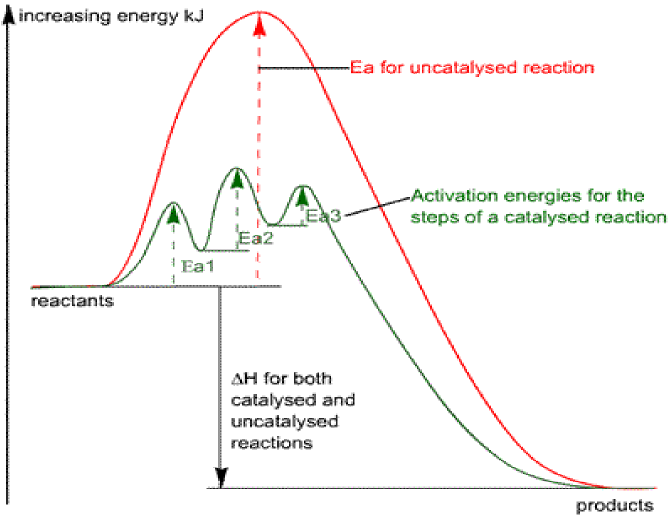

Figure 3. Schematic representation of the energetics in a catalytic cycle.

A catalyst reduces the activation energy of a reaction in two ways. First of all, it bonds with one or more of the reactants and so reduces the energy needed by the reactant molecules in order to finish the reaction. Secondly, it brings the reactants together and holds them in a way that makes reaction more likely. This new appropriate orientation for the reaction reduces the entropy which increases the possibility of the reaction occurrence. It is noteworthy that the catalyst has not any affect the overall entropy change for the reaction.

It only creates a new and easier pathway to the reaction. This pathway may compose of one or more steps which we call the mechanism of the reaction.

The catalytic efficiency of the catalyst can be measured by determining its catalytic turnover frequency, TOF given by the Equation 4 where ν is the rate of the reaction and |Q| is the mole of the catalyst. A highly active catalyst, one that results in a fast reaction even in low concentrations, has a large turnover frequency.

$$\mathrm{TOF} = \frac{\mathrm{v}}{|\mathrm{Q}|} \qquad (4)$$

Another factor that helps determining catalytic efficiency is the catalytic turnover number, TON. This term can be defined as the number of catalytic cycles for a given process and represented as moles of product per moles of catalyst for a given reaction.

Besides being an effective catalyst, it should be also selective. Whether it is homogeneous or heterogeneous; the catalyst should increase the rate of the reaction with producing high amount of desired product and minimum amount of side product in a chemical reaction.

Catalyst size is the other key factor to consider a catalyst as effective. Particles in the 1-10 nm range create a new vision in surface chemistry because surface-reactant interactions can become stochiometric. As shown in Figure 4, when the size of the particle decreases, surface area of the material increases allowing good ‘atom economy’ in surface-gas, surface-liquid, or even surface-solid reactions.

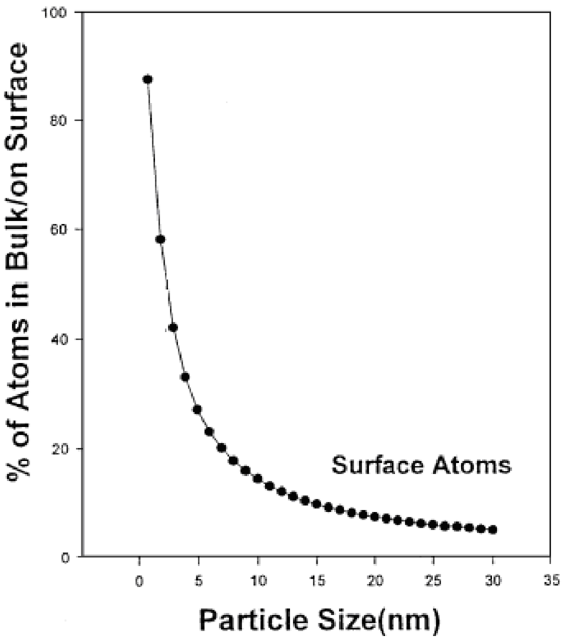

Figure 4. Calculated surface to bulk atom ratios for spherical iron nanoparticles (Taken from the reference [61]).

It is important to consider that a 3 nm particle has 50% of the atoms on the surface, while a 20 nm particle has fewer than 10%. This indicates that it is crucial to get smaller particles in order to benefit from the atom economy desired. It is shown in Figure 5 clearly that the percentage of edge and corner atoms also increases with reducing size and this is the reason of small particles are preferred as catalyst. As size changing, intrinsic properties of materials; moreover the properties of nanoparticles also change. With changing band gaps, coercive force in magnetic materials can be manipulated, there is a reduction in melting points, surfaces becomes more reactive, and nanostructural metal specimens can have enhanced hardness by a factor [62] compared to bulk metals.

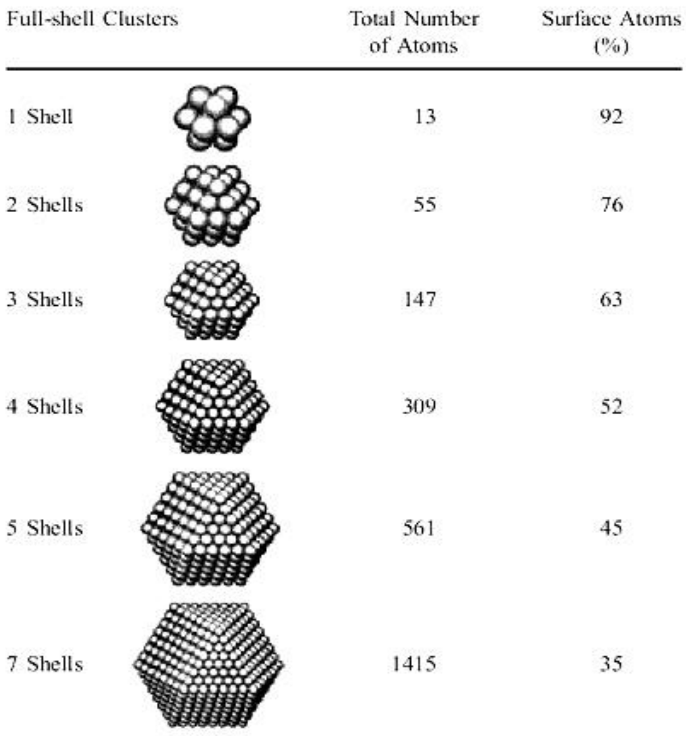

Full-shell Clusters	Total Number of Atoms	Surface Atoms (%)
1 Shell	13	92
2 Shells	55	76
3 Shells	147	63
4 Shells	309	52
5 Shells	561	45
7 Shells	1415	35

Figure 5. The relation between the total number of atoms in full shell clusters and the percentage of surface atoms.

3.2. Transition Metal(0) Nanoclusters

Colloidal nanoclusters are mono dispersed particles with diameter size less than 10nm [63]. They have distinctive properties arise from the fact that when a metal particle with bulk properties is reduced to the nanometer size scale, the density of states in the valence and the conduction band decreases to such an extent that the quasi-continuous density of states is replaced by a discrete energy level structure and the electronic properties change dramatically so these particles and their properties lie somewhere between those of bulk and single-particle species [64,65].

Because of these unique properties, they have variety of applications including quantum dots [66], quantum computers [67], quantum devices [68], chemical sensors [69], light-emitting diodes [70], ferrofluids for cell separations [71] and photochemical pattern applications such as flat-panel displays [72]. Among the variety of usage area of transition metal nanoclusters discussed above, catalysis is of great interest because of their high surface to volume ratio and a unique combination of reactivity, stability, and selectivity. They have large percentage of metal atoms laying on its surface. Moreover because of quantum size effect the electrons in nanoclusters are confined to spaces that can be as small as a few atom widths across [73] which lead to control ability both the nanocluster size and the surface ligands in a quantitative, modifiable manner.

3.3. Synthesis of Transition Metal Nanoclusters

There are several synthetic methods which have been used for the preparation of transition metal nanoclusters. These methods can be divided into two methods: physical methods, also known as top-down, and chemical methods, also known as bottom-up [74]. The synthesized nanoparticles need to be stabilized since they are not thermodynamically stable. The list of preparation methods some examples of these methods and stabilizing techniques used are given below [64].

3.3.1. Chemical Reduction of Metal Salts

This method is the most commonly used method for synthesizing colloidal suspensions of metal from its metal salt precursor. The reducing agent could be prepared via in-situ -mostly in aqueous systems- or the solvent and reducing agent can be one and the same - in non-aqueous systems- [64]. Hydrogen, carbon monoxide, hydrides, salts such as sodium borohydride, ammonia borane and sodium citrate, moreover oxidizable solvents such as alcohols are the examples of reducing agents [74].

3.3.1.1. Hydrogen Reduction

Heretofore, various transition metal salts such as chloride salts of Au, Ag, Ir, Pt, Pd, Rh, and Ru have been reduced by hydrogen, and stabilized by PVA (polyvinylacetate) in order to prepare aqueous colloidal solution [75].

3.3.1.2. Chemical Hydrides

There are several chemical hydrides used in this method to prepare nanoclusters. Among them the borohydrides ($NaBH_4$ or KBH_4) are widely used in hydride reduction method generating aqueous suspensions of metals from their metal salts. Ru(0) nanoparticles were prepared in the presence of acetate stabilizer using this approach [24]. Moreover, $NaBH_4$ reduction was used to obtain Au, Ag, Pt, Pd, and Cu nanoparticles stabilized by dendrimers (polyamidoamine or PAMAM) [76,77,78] which help to obtain almost monodispersed particles.

3.3.1.3. Alcohols

By alcohol refluxing method various transition metal salts could be reduced. In this method, the alcohol behaves as solvent and reducing agent. The alcohols having α-hydrogen such as methanol, ethanol and 2-propanol act as reducing agents. In the reduction process, the alcohols are oxidized to the corresponding carbonyl compounds shown in Figure 6. In the presence of water that reaction tends to be more effective [74].

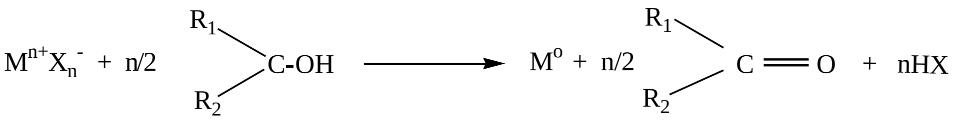

Figure 6. Metallic nanoparticles formation in alcohol medium.

Rh, Pt, Pd, Os, or Ir transition metal nanoparticles are synthesized by using aqueous alcohols as reducing agents [79,80,81,82,83].

3.3.2. Thermolysis

Main principle of this method is that many organometallic compounds of transition metals are potential sources of nanoparticle precursors since they tend to decompose thermally to their metals. With this applicable method, carbonyl-containing complexes of rhodium, iridium, ruthenium, osmium, palladium and platinum in polymer solutions have been synthesized [84].

Using palladium acetate, palladium acetylacetonate and platinum acetylacetonate as precursor these metals' organols were also prepared via thermolysis in high boiling point organic solvents [85,86]. The obtained organols are not small since these preparations have been performed without stabilizing agents.

3.3.3. Radiolysis and Photolysis

Photochemical methods can be divided into two groups. First one is the reduction of metal salt precursor by solvated electrons and free radicals which is a radiolytic method. Second one is the photolysis of photolabile metal complexes. Radiolytic methods have an advantage of formation of colloidal particles with a large number of highly homogen disperse metal nuclei [64].

3.3.4. Displacement of Ligands From Organometallic Complexes

Reduction of metals can be accomplished before colloid preparation, giving a zerovalent metal complex as a precursor. As a case in this point, the synthesis of metal carbonyls and their thermolysis in nanoparticles preparation are achieved with this approach [87].

3.3.5. Reduction by Electrochemical Methods

In this method, for metal source a sacrificial anode is used and it acts both as reducing agent and stabilizing agent as a result of its oxidation with a stabilizer present in the solution. The ions formed then reduced at the cathode to generate metallic nanoparticles. The process is accomplished by this order: (i) dissolution of the anode to form metal ions, (ii) migration of the metal ions to cathode, (iii) reduction of the metal ions at the surface of the cathode, (iv) aggregation of the particles by stabilizing agent around the metal cores then (v) precipitation of the metal nanoparticles. It is a large scale method that allows synthesis of size controlled colloids.

3.4. Stabilization of Metal Nanoparticles in Liquids

As stated before, synthesized metal nanoparticles need to be stabilized against to agglomeration because of their thermodynamical instability. At short interparticle distance, two particles attracted each other by Van der Waals forces and in the absence of repulsive forces two counteract this attraction an unprotected sol would coagulate. This counteraction can be achieved by two methods, electrostatic stabilization and steric stabilization [88].

3.4.1. Electrostatic Stabilization

In this stabilization technique colloidal metal particles are surrounded by an electrical double layer formed by adsorbed anions and cations which are attracted to them. It is a coulombic repulsion between particles, and the net result is shown schematically in Figure 7. To illustrate, gold sol particles generated reduction of aqueous $[AuCl_4]^-$ in the presence of citrate and chloride anions and cations that are used for stabilizing purpose [89] could be given.

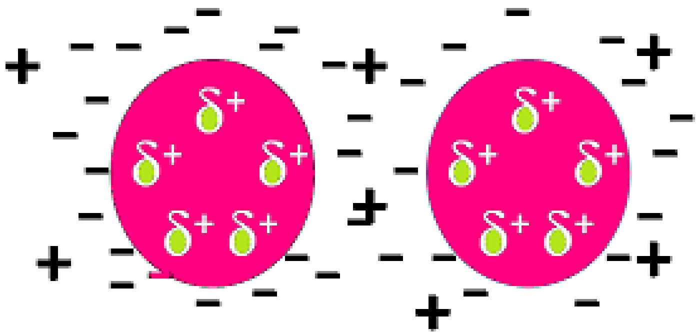

Figure 7. Schematic representation of electrostatic stabilization of metal colloid particles.

It is a fact that the coulombic repulsion between the particles decays nearly exponentially with the particle distance and the weak in minimum potential energy is the key factor of stability. So if the electric potential created by double layers is high enough, electrostatic repulsion prevents aggregation [90].

3.4.2. Steric Stabilization

In this method, a protective layer is formed by the adsorption of big molecules such as polymers, surfactants or ligands to the surface of the nanoparticles (Figure 8).

Figure 8. Schematic representation of steric stabilization of metal nanoparticles.

A steric protectant should coordinate to the metals' particle surface effectively and should disperse and dissolved by the solvent used in the reaction. A widely used protectant, polymers, is chosen according to those circumstances in order to stabilize colloidal particles effectively [64].

3.5. Characterization of Metal Nanoparticles

The size, structure and the composition are the three important features of colloidal metal nanoparticles need to be defined. In order to have a full image of a metal nanoparticle there should be more than one technique characterizing this nanoparticle.

Transmission electron microscopy (TEM) or high resolution transmission electron microscopy (HRTEM) is the most common used technique to characterize nanoparticles. This technique provides visual information about nanoparticles including morphology, dimension, size distribution and structure. Another method giving information about size of a nanoparticle is X-Ray electron diffraction (XRD) technique. Using peak features and Debye- Scherrer equation one can calculate the approximate nanoparticle size. Other commonly used methods for characterization of metal particles include UV-Visible spectroscopy (UV-Visible), nuclear magnetic resonance spectroscopy (NMR), infrared spectroscopy (IR), elemental analysis, and energy dispersive spectroscopy (EDS). Analytical ultracentrifugation-sedimentation, extended X-ray absorption fine structure (EXAFS), scanning tunneling microscopy (STM), atomic force microscopy (AFM), high performance liquid chromatography (HPLC), light scattering, time of flight mass spectroscopy, magnetic susceptibility and electrophoresis or ion-exchange chromatography are the other methods used with less popularity. Figure 9 gives an overall picture of the methods widely used in the characterization of nanoparticles [91].

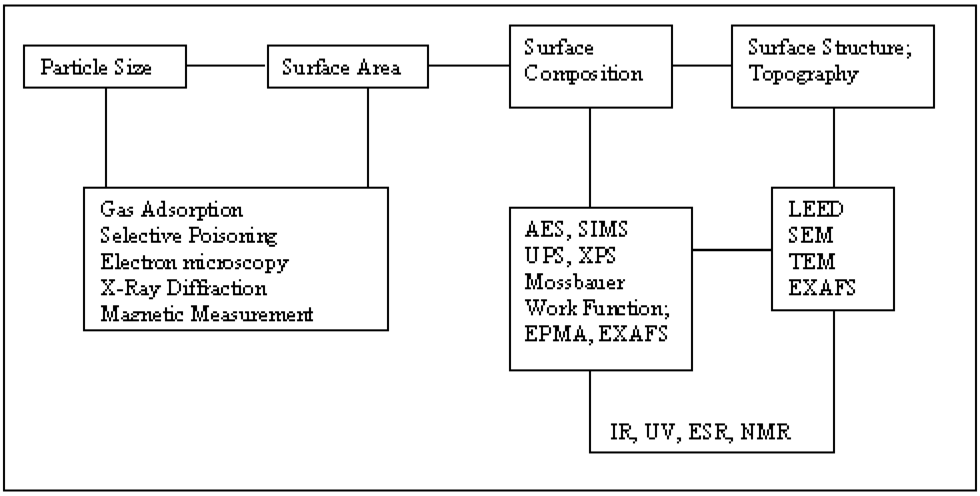

Figure 9. Schematic representation of common methods for characterization of nanoparticles.

CHAPTER 4

EXPERIMENTAL

4.1. Materials

Palladium(II) acetylacetonate (99%), Ruthenium(III) chloride ($RuCl_3$) (45-55%), borane-ammonia complex (> 97%), poly(N-vinyl-2-pyrrolidone) (PVP-40, average molecular weight 40 000) were purchased from Aldrich® and used as received. Methanol was purchased from Riedel-De Haen AG Hannover, and it was distilled over metallic magnesium. All methanolysis reactions were performed using the distilled methanol under inert gas atmosphere unless otherwise specified. Teflon coated magnetic stir bars and all glassware were cleaned with acetone and dried in an oven at 150 ^{o}C.

4.2 In-Situ Generation of PVP-Stabilized Palladium(0) Nanoclusters in the Methanolysis of Ammonia-Borane

“Both the in situ formation of PVP-stabilized palladium(0) nanoclusters and the catalytic methanolysis of AB were performed in the same medium. Before starting the experiment, a jacketed reaction flask (50 mL) containing a Teflon-coated stir bar was placed on a magnetic stirrer (IKA® RCT Basic) and thermostated to 25.0 ± 0.5 °C by circulating water through its jacket from a constant temperature bath (Lauda RL6)” [59].

“Then, a glass graduated cylinder tube filled with water was connected to the Schlenk tube to measure the volume of the hydrogen gas evolving from the reaction. Next, 1.55 mg palladium(II) acetylacetonate (0.5 mM Pd) and 2.78 mg PVP-40 (2.5 mM) was dissolved in 5 mL methanol in the Schlenk tube with a stir bar and let them stir. Then, 64 mg ammonia-borane (200 mM AB) was dissolved in 5 mL methanol elsewhere and transferred into the Schlenk tube under argon atmosphere at 700 rpm with a constant stirring. The initial concentrations of AB and palladium were 200 mM AB, and 0.5 mM Pd, respectively. A molar ratio of AB to metal precursors greater than 100 was used to ensure complete reduction of Pd^{2+} to its zero oxidation state and to observe the catalytic hydrolysis of AB at the same time. The formation of nanoclusters took less than 1 minute and immediate hydrogen gas evolution took place, indicating that nanoclusters formed start to catalyze the methanolysis of AB. Catalytic methanolysis was monitored by measuring the volume of hydrogen gas evolved every 2 minutes at constant pressure by determining the decrease in the water level of glass tube which was connected to the Schlenk tube (Figure 10)” [59].

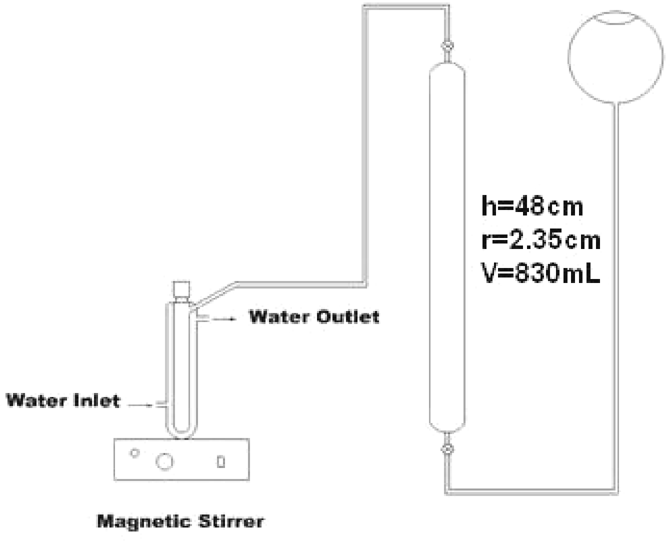

Figure 10. The experimental setup used in performing the catalytic methanolysis of ammonia-borane and measuring the hydrogen generation rate.

“In a control experiment, stirring rate was varied in the range 0-800 rpm. It was found that after 700 rpm the stirring rate has no significant effect on the catalytic activity. This indicates that system is in a non-MTL (mass transfer limitation) regime at stirring rate > 700 rpm. In other words, there is no diffusion problem due to the presence of the polymer in concentration less than 5 mM” [59].

4.3. In-Situ Generation of PVP-Stabilized Ruthenium(0) Nanoclusters in the Methanolysis of Ammonia-Borane

The catalytic activity of PVP-stabilized ruthenium(0) nanoclusters in the methanolysis of ammonia-borane was determined by measuring the rate of hydrogen generation. To determine the rate of hydrogen generation, the catalytic methanolysis of ammonia-borane were performed in Parr-5101 low-pressure reactor equipped with circulating water-bath for constant temperature control, and mechanical stirrer. The Parr-5101 low-pressure reactor was connected with a digital transmitter to a computer using RS-232 module. The progress of an individual methanolysis reaction was followed by monitoring the increase in the pressure of hydrogen gas with the program Calgrafix. The temperature was also controlled via thermocouple within the reactor with the Calgrafix program. The pressure vs. time data was processed using Microsoft Office Excel 2007 and Origin 7.0, and then converted into the values in the proper unit, volume of hydrogen (mL) (Figure 11).

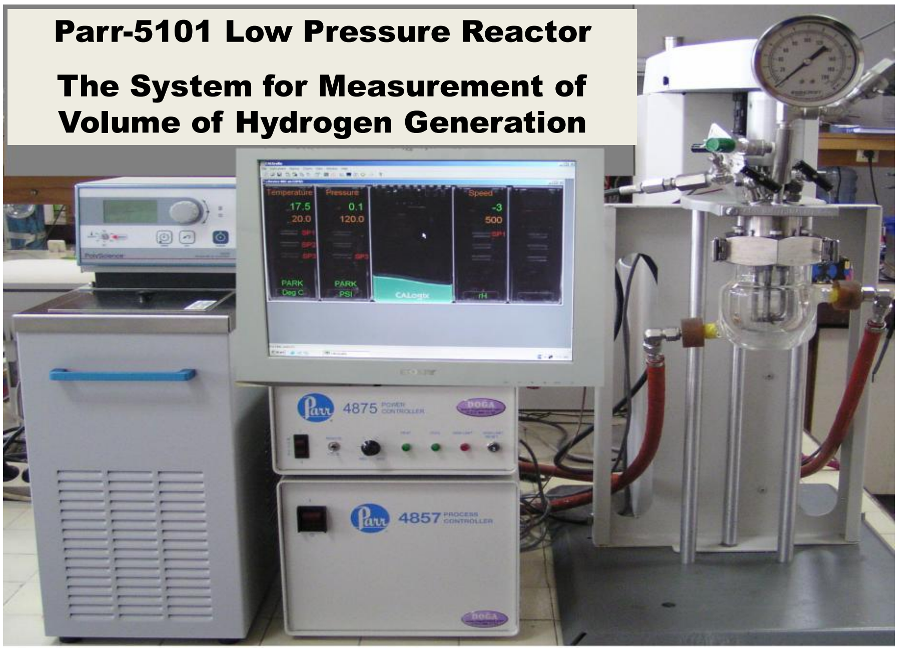

Figure 11. The Parr-5101 Low Pressure Reactor used in performing the catalytic methanolysis of ammonia-borane and measuring the hydrogen generation rate.

Before starting the catalytic activity test experiments, the reactor (300 mL) was thermostated at 25.0 ± 0.5 ºC. In a typical experiment, 46 mg $RuCl_3$ was dissolved in 20 mL methanol in order to prepare stock solution of $RuCl_3$ (5 mM). To study with 1.5 mM catalyst, 3 mL of the stock solution was transferred with a glass pipette into the reactor. As a stabilizer, 33.3 mg PVP (1:20 = metal:polymer) was added to the reactor and let them to mix about 3min. Then, 64 mg (200 mM) H_3NBH_3, which acts both reducing agent and substrate, were dissolved in 7 mL methanol and added to PVP-Ru solution. The stirring rate of the magnetic stirrer was set to 700 rpm. In a control experiment, the stirring rate was varied in the range 0 –1000 rpm. It was found that after 700 rpm, the stirring rate has no significant effect on the catalytic activity. This indicates that the system is in a non-MTL (mass transfer limitation) regime at stirring rates after 700 rpm. In other words, there is no diffusion problem due to the presence of the polymer.

In addition to the volumetric measurement of the hydrogen evolution, the conversion of ammonia borane to ammoniummethoxytetraborate was also checked by ^{11}BNMR spectra of the solution.

4.4. Self-Methanolysis of Ammonia-Borane

“64 mg AB were dissolved in 10 mL methanol in a jacketed reaction flask (50 mL) containing a Teflon-coated stir bar. The reaction flask was thermostated to a temperature in the range of 15-35 °C by circulating water through its jacket from a constant temperature bath. The experiment was started simultaneously by closing the reaction flask and turning on the stirrer at 700 rpm. Then the reaction was followed by measuring volume of hydrogen liberating” [59].

4.5. Instrumentation

4.5.1. Characterization of PVP-Stabilized Palladium(0) Nanoclusters

4.5.1.1. TEM (Transmission Electron Microscopy)

“The TEM and selected area electron diffraction (SAED) images were obtained using a JEM-2010 (JEOL) TEM instrument operating at 200 kV. The samples used for the TEM experiments were harvested from the in-situ generation of PVP-stabilized palladium(0) nanoclusters solution as described above. The nanoclusters solution was centrifuged at 8000 rpm for 8 minutes. The separated nanoclusters were washed with acetone to remove the excess PVP and other residuals. Then, the nanoclusters sample was redispersed in 5 mL methanol. One drop of the colloidal solution was deposited on the silicon oxide coated copper grid and evaporated under inert atmosphere. Samples were examined at magnifications between 100 and 400 K” [59].

4.5.1.2. XPS (X-Ray Photoelectron Spectroscopy)

“The samples used for X-ray photoelectron spectroscopy (XPS) analysis were prepared by evaporating the methanol from the nanoclusters solution, as described in the section 4.2, by rotary evaporation under vacuum. The resulting solid particles were washed with acetone to remove the residuals from the solid sample under N_2 atmosphere. X-ray photoelectron spectrum was taken by using a SPECS spectrometer equipped with a hemispherical analyzer and using monochromatic Al-Kα radiation (1450 eV, the X-ray tube working at 15 kV and 350 W) and pass energy of 48 eV. To better access the metal core in the sample by scraping off the polymer matrix from the surface, the polymer matrix was scraped from surface of the sample via bombardment by argon ions at 3000 eV for 3 minutes” [59].

4.5.1.3. FT-IR (Fourier Transform Infrared) Spectroscopy

“The sample prepared for the XPS analysis was also used for FT-IR analysis. FT-IR spectra of neat PVP and PVP-stabilized palladium(0) nanoclusters were taken from KBr pellet on a Bruker-Advance FTIR Spectrophotometer using Opus software” [59].

4.5.1.4. ^{11}B NMR (Nuclear Magnetic Resonance) Spectroscopy

“To examine the final reaction product by ^{11}B-NMR, a certain amount of sample was taken directly from the Schlenk tube into quartz NMR tube after the stochiometric hydrogen generation from the catalytic methanolysis of AB finished. A few drops of $CDCl_3$ solution were added into the quartz NMR tube. ^{11}B-NMR spectra were recorded on a Bruker Avance DPX 400 with an operating frequency of 128.15 MHz for ^{11}B” [59].

4.5.1.5. UV-Vis. (Ultraviolet Visible Spectroscopy) Study

“UV-Vis electronic absorption spectra of palladium(II) acetylacetonate and PVP-stabilized palladium(0) nanoclusters were recorded in methanol solution on a Varian-Carry100 double beam instrument” [59].

4.5.1.6. XRD (X-ray Diffraction)

“X-ray diffraction (XRD) patterns of PVP-stabilized palladium(0) nanoclusters were recorded on a Rigaku Miniflex diffractometer with CuKα (30 kV, 15 mA, λ= 1.54051 Å), over a 2θ range of 5 to 90 ° at room temperature” [59].

4.5.2. Characterization of PVP-Stabilized Ruthenium(0) Nanoclusters

4.5.2.1. TEM (Transmission Electron Microscopy)

JEM-2010 (JEOL) TEM instrument operating at 200 kV used for TEM measurement. The samples used for the TEM experiments were taken from the in situ-generated PVP-stabilized ruthenium(0) nanocluster solution described previously. The nanocluster solution was centrifuged at 8000 rpm for 8 min. The separated nanoclusters were washed with acetone to remove the excess PVP and other residuals. Then, the nanocluster sample was redispersed in 5 mL methanol. One drop of the colloidal solution was deposited on the silicon oxide coated copper grid and evaporated under inert atmosphere. Samples were examined at magnifications between 100 and 400 K.

4.5.2.2. XPS (X-Ray Photoelectron Spectroscopy)

X-ray photoelectron spectrum (XPS) was taken by using SPECS spectrometer equipped with a hemispherical analyzer and using monochromatic Mg-Kα radiation (1250 eV, the X-ray tube working at 15 kV and 350 W) and pass energy of 48 eV. To get better result, the metal core in the sample by scraping off the polymer matrix from the surface, the sample surface was bombardment by argon ion by passing 3000 eV energy for 3 minutes.

4.5.2.3. FT-IR (Fourier Transform Infrared) Spectroscopy

The sample prepared for the XPS analysis was also used for FT-IR analysis. FT-IR spectra of neat PVP and PVP-stabilized ruthenium(0) nanoclusters were taken from KBr pellet on a Bruker-Advance FTIR Spectrophotometer using Opus software.

4.5.2.4. ^{11}B NMR (Nuclear Magnetic Resonance) Spectroscopy

To define the final reaction product by ^{11}B-NMR, a certain amount of sample were taken directly from the reactor into quartz NMR tube after the stochiometric hydrogen generation from the catalytic methanolysis of AB finished. Then a few drops of $CDCl_3$ solution were added into the quartz NMR tube. ^{11}B NMR spectra were recorded on a Bruker Avance DPX 400 with an operating frequency of 128.15 MHz for ^{11}B.

4.5.2.5. UV-Vis. (Ultraviolet Visible Spectroscopy) Study

UV-Vis electronic absorption spectra of ruthenium(III) chloride and PVP-stabilized ruthenium(0) nanoclusters were recorded in methanol solution on Varian-Carry100 double beam instrument.

4.5.2.6. XRD (X-ray Diffraction)

X-ray diffraction (XRD) pattern of PVP-stabilized ruthenium(0) nanoclusters were recorded on a Rigaku Miniflex diffractometer with CuKα (30 kV, 15 mA, λ= 1.54051 Å), over a 2θ range from 5 to 90 ° at room temperature.

4.6. Hg-Poisoning in the Methanolysis of Ammonia-Borane Catalyzed by PVP-Stabilized Palladium(0) Nanoclusters

“A standard nanocluster formation and methanolysis experiment was started with 200 mM AB, 1.0 mM palladium(II) acetylacetonate and 5.0 mM PVP in 10 mL methanol at 25 ± 0.5 °C. After about 40% conversion of AB, elemental Hg ([Hg]/[Pd]=300 equiv.) was added to the solution under stirring. The reaction was followed further for 3 h” [59].

4.7. Hg-Poisoning in the Methanolysis of Ammonia-Borane Catalyzed by PVP-stabilized Ruthenium(0) Nanoclusters

A standard nanocluster formation and methanolysis experiment was started with 400 mM AB, 1.5 mM ruthenium(III) chloride and 30 mM PVP in 10 mL methanol at 25 ±0.5 °C. After about 40% conversion of AB, elemental Hg ([Hg]/[Ru]=350) was added to the solution under stirring. The reaction was followed for a further 3 h.

4.8. Kinetics of the Methanolysis of Ammonia-Borane Catalyzed by PVP-Stabilized Palladium(0) Nanoclusters

“In order to determine the rate law of the methanolysis of AB catalyzed by PVP-stabilized palladium(0) nanoclusters, three different sets of experiments were performed as described in the ‘In-situ generation of PVP-stabilized palladium(0) nanoclusters in the methanolysis of ammonia-borane' section. Firstly, AB concentration was kept constant at 200 mM and the palladium concentration was varied in the range of 0.5, 0.75, 1.0, 1.25, and 1.5 mM" [59].

"In the second set of experiments, palladium concentration was kept constant at 0.5 mM and the AB concentration was varied in the range of 100, 150, 200, 250, and 300 mM. In the third set, the methanolysis reaction was performed at constant catalyst (1 mM Pd) and constant AB (200 mM) concentration by varying the temperature in the range of 15-35 °C to obtain the activation parameters; activation energy (Ea), entalphy ($\Delta H^{\neq}$) and entropy ($\Delta S^{\neq}$)" [59].

4.9. Kinetics of the Methanolysis of Ammonia-Borane Catalyzed by PVP-Stabilized Ruthenium(0) Nanoclusters

In order to determine the rate law of the methanolysis of AB catalyzed by PVP-stabilized ruthenium(0) nanoclusters, three different set of experiments were performed as described in section 'In Situ Preparation of PVP-stabilized Ruthenium(0) Nanoclusters in the Methanolysis of Ammonia Borane'. Firstly, AB concentration was kept constant at 200 mM varying the ruthenium concentration 0.5, 1.0, 1.5, 2.0 and 2.5 mM. In the second set, ruthenium concentration was kept constant at 1.5 mM varying the AB concentration in the range of 0.1 M- 5 M. In the third set, the methanolysis reaction was performed at constant catalyst (1.5mM Ru) and constant AB (200 mM) concentration varying the temperature in the range of 15-35 °C to obtain the activation parameters; activation energy (Ea), entalphy ($\Delta H^{\neq}$) and entropy ($\Delta S^{\neq}$).

4.10. Determination of the Catalytic Lifetime of PVP-Stabilized Palladium(0) Nanoclusters in the Methanolysis of Ammonia-Borane

“The catalytic lifetime of PVP-stabilized palladium(0) nanoclusters in the methanolysis of AB was determined by measuring the total turnover number (TTON). Such a lifetime experiment was started with a 20 mL solution containing 0.5 mM palladium(II) acetylacetonate and 500 mM AB (320 mg) at 25 ± 0.5 °C. After all conversion of added H_3NBH_3 completed by checking stochiometric H_2 gas evolution (3.0 mol H_2/mol H_3NBH_3), a new batch of 320 mg ammonia-borane added and the reaction was kept going in this way until no hydrogen gas evolution was observed. The ammonia generation during the TTO experiments was checked before addition of new batch of AB by using an acid/base indicator” [59].

4.11. Determination of the Catalytic Lifetime of PVP-Stabilized Ruthenium(0) Nanoclusters in the Methanolysis of Ammonia-Borane

The catalytic lifetime of PVP-stabilized ruthenium(0) nanoclusters in the methanolysis of AB was determined by measuring the total turnover number (TTON). Such a lifetime experiment was started with a 20 mL solution contain 0.125 mM ruthenium (III) chloride and 200 mM AB (128 mg) at 25 ± 0.5 °C. After all conversion of added H_3NBH_3 completed by checking stochiometric H_2 gas evolution (3.0 mol H_2/mol H_3NBH_3), a new batch of 128 mg ammonia-borane added and the reaction was kept on in this way until no hydrogen gas evolution was observed. The ammonia generation during the TTO experiments was checked before addition of new batch of AB by using acid/base indicator.

CHAPTER 5

RESULTS AND DISCUSSION

5.1. In-Situ Generation and Characterization of PVP-Stabilized Palladium(0) Nanoclusters

“PVP-stabilized palladium(0) nanoclusters were formed in-situ from the reduction of palladium(II) acetylacetonate in the presence of PVP during the methanolysis of AB. In a typical experiment, polymer and metal precursor were first mixed well in methanol by stirring at 700 rpm and then AB was added to the reaction solution in order to form palladium(0) nanoclusters. As the other amine-boranes [19], AB acts as reducing agent and provides two electrons for the reduction of Pd(II) to Pd(0). Then, the Pd(0) nanoclusters are formed by the nucleation and autocatalytic growth mechanism [92]. The abrupt colour change from pale yellow to dark brown after addition of AB solution into the mixture of metal precursor and PVP indicates the formation of PVP-stabilized palladium(0) nanoclusters. Concomitantly, hydrogen evolution starts after the colour change indicating that the nanoclusters are the active catalyst in the methanolysis of AB” [59].

“The conversion of palladium(II) acetylacetonate to palladium(0) nanoclusters can nicely followed by the UV-visible electronic absorption spectra taken during the reaction (Figure 12)” [59].

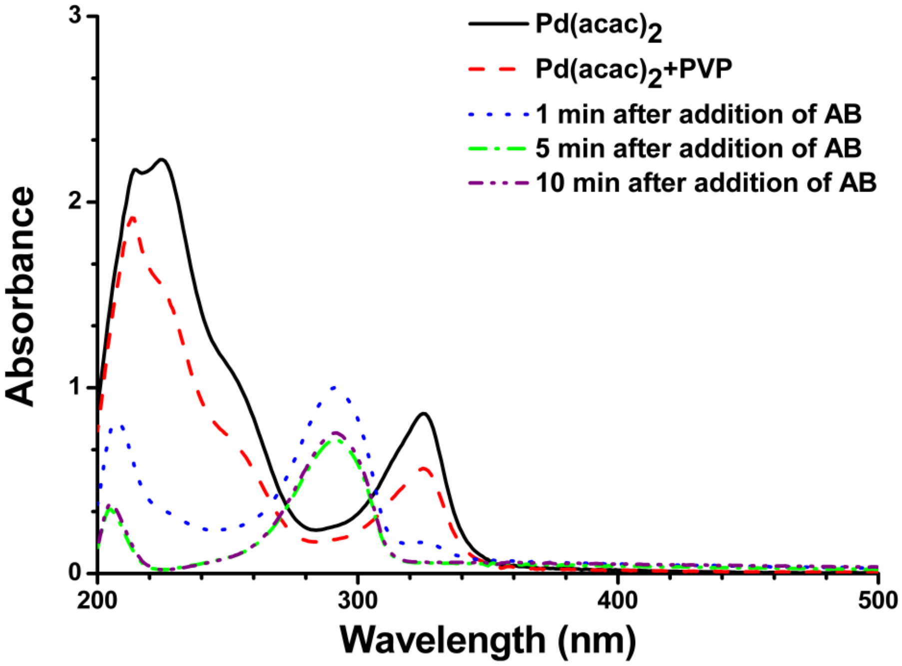

Figure 12. UV-Visible electron absorption spectra taken during the reaction of palladium(II) acetylacetonate with ammonia-borane in the presence of PVP in methanol solution.

“The absorption bands of palladium(II) acetylacetonate at 330, 260 and 225 nm gradually disappear upon addition of AB into the solution while a new absorption band at 295 nm grows in concomitantly. The latter band is attributable to Pd(0) nanoclusters [93]. This spectroscopic observation indicates that the reduction of palladium(II) to palladium(0) is completed within less than 5 min” [59].

“Survey experiments performed by varying the polymer to metal ratio in the range of 1:1 - 5:1 showed that the highest stability and catalytic activity of the PVP-stabilized palladium(0) nanoclusters are obtained when a five-fold molar excess of polymer is used in the methanolysis of AB. It is most likely that the complete dissolution of PVP in methanol achieved by vigorous stirring for long time is required for obtaining stable palladium(0) nanoclusters ” [59].

“The PVP- stabilized palladium(0) nanoclusters are highly stable in solution even for months and they can be isolated from the solution as solid materials by removing the volatiles in vacuum. The solid palladium(0) nanoclusters isolated are also stable for months under inert atmosphere and readily redispersible in methanol. Moreover, when redispersed in methanol, the palladium(0) nanoclusters still show catalytic activity in methanolysis of AB” [59].

“The morphology and particle size of the PVP-stabilized palladium(0) nanoclusters were studied by taking the TEM image (Figure 13 a). Palladium(0) nanoclusters in average particle size of 3.2 ± 0.5 nm are obtained as shown in the histogram (Figure13 b)” [59].

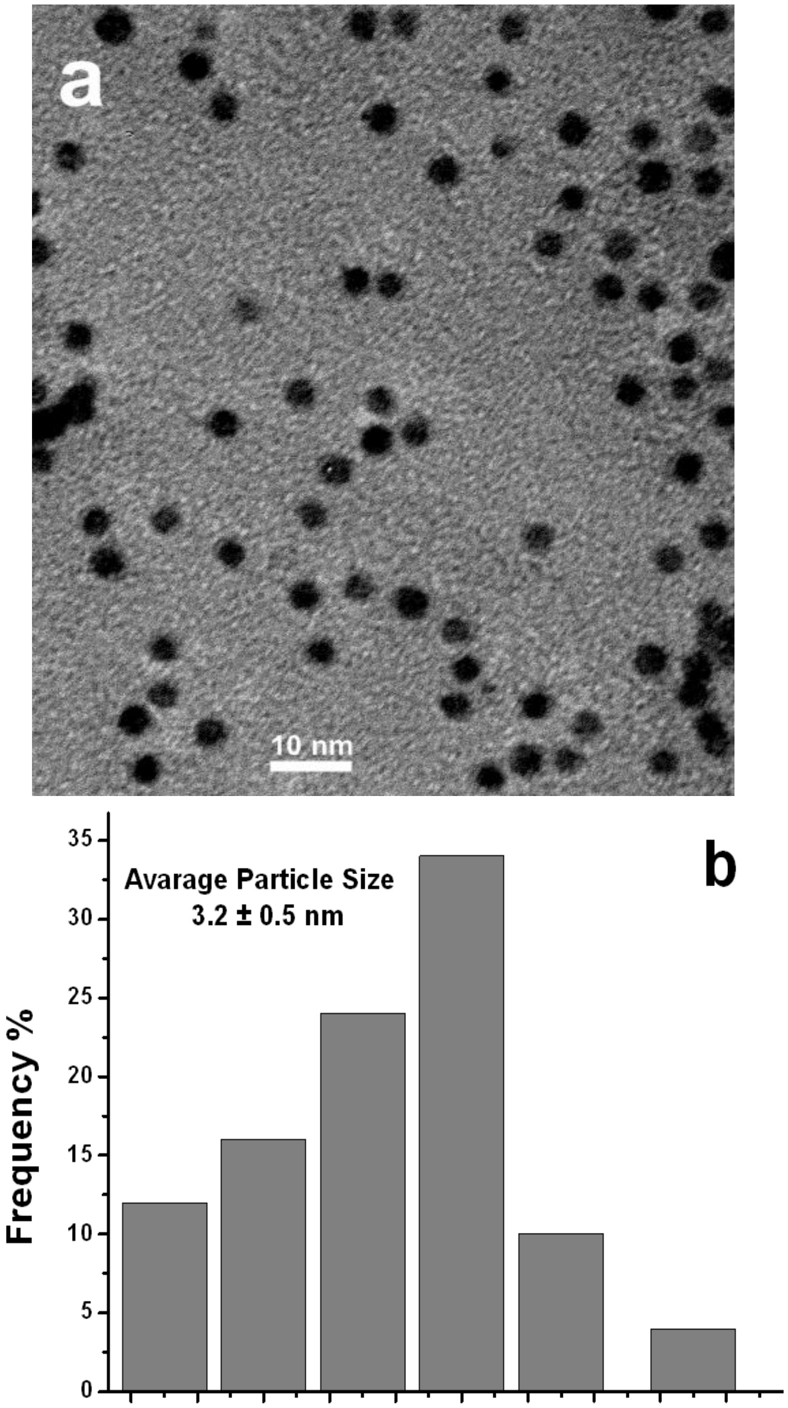

Figure 13. (a) TEM image and (b) associated histogram for PVP-stabilized palladium(0) nanoclusters formed from the reduction of palladium(II)acetylacetonate (0.5 mM) by ammonia-borane (200 mM) in the presence of PVP (2.5 mM).

“The nanoclusters are in spherical shape with no agglomeration. They show similar particle dispersion and shape with the PVP-stabilized palladium nanoparticles prepared by using well-known alcohol reduction method, but they have a bigger particle size [28]. The use of mild reducing agent AB and low temperature might lead to formation of palladium nanoclusters with a bigger particle size. However, our nanoclusters catalysts have a narrover particle size distribution and a smaller particle size than nanoparticles used as catalysts for the methanolysis of AB [21], which is important issue on higher catalytic activity” [59].

“The XPS spectrum of PVP-stabilized palladium(0) nanoclusters given in Figure 14 shows two well resolved peaks at 335.8 and 341.4 eV, readily assigned to the Pd(0) $3d_{5/2}$ and Pd(0) $3d_{3/2}$, respectively, by comparing to the values of metallic palladium” [94, 59].

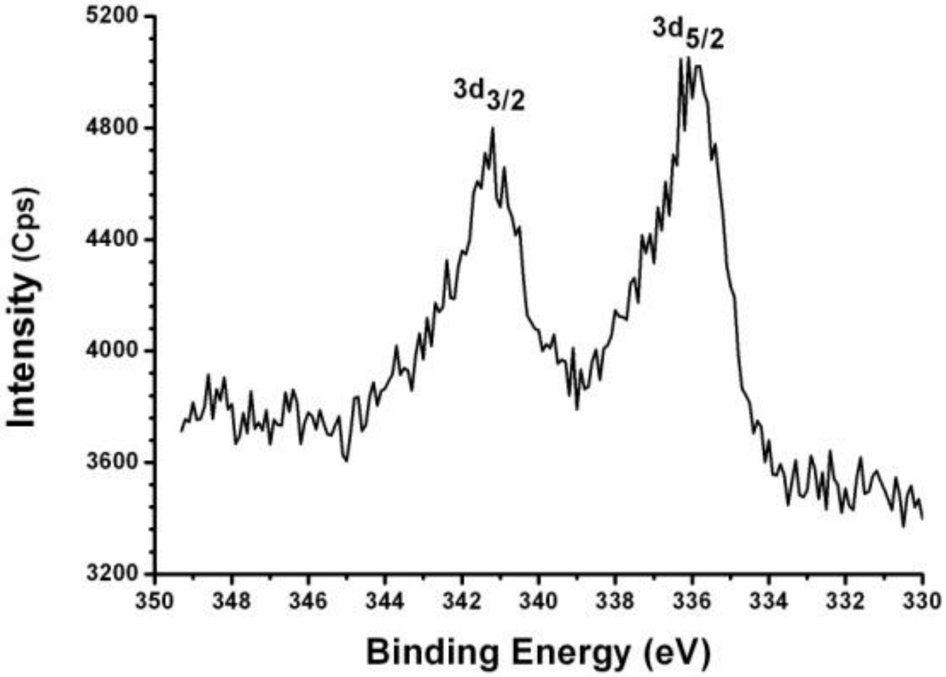

Figure 14. X-Ray photoelectron spectrum of PVP-stabilized palladium(0) nanoclusters isolated from the reduction of palladium(II) acetyl acetonate (0.5 mM) by ammonia-borane (200 mM) in the presence of PVP (2.5 mM).

“That no higher oxidation peak for palladium is observed in the XPS spectrum might be due to protection of palladium(0) by the surface adsorbed PVP against oxidation during the sample preparation. Also, comparison of the FT-IR spectra of the PVP-stabilized palladium(0) nanoclusters and neat PVP (Figure 15), taken from KBr pellet, shows the existence of PVP in the nanoclusters sample, most probably both for adsorbed on the surface of nanoclusters and for free PVP molecules due to high polymer to metal ratio is needed to stabilize palladium(0) nanoclusters” [59].

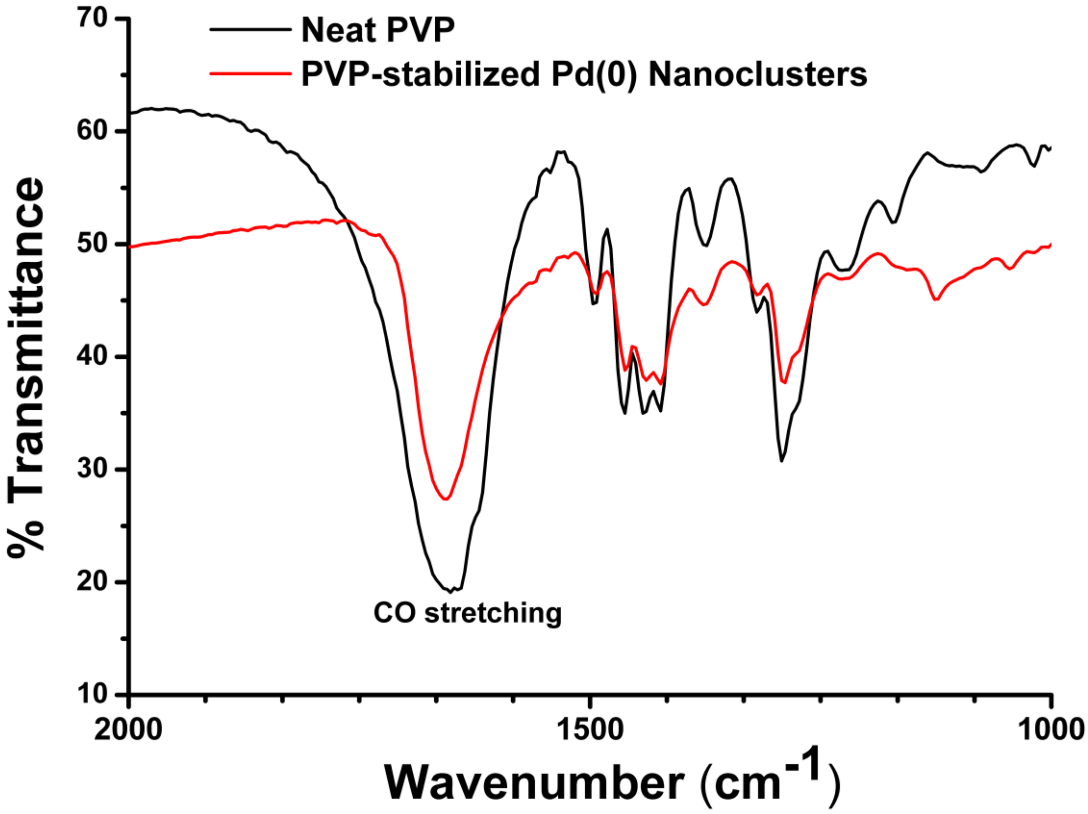

Figure 15. FT-IR spectra of the PVP-stabilized palladium(0) nanoclusters and neat PVP. The PVP-stabilized palladium(0) nanoclusters were isolated from the reduction of palladium(II) acetylacetonate (0.5 mM) by AB (200 mM) in the presence of PVP(2.5 mM).

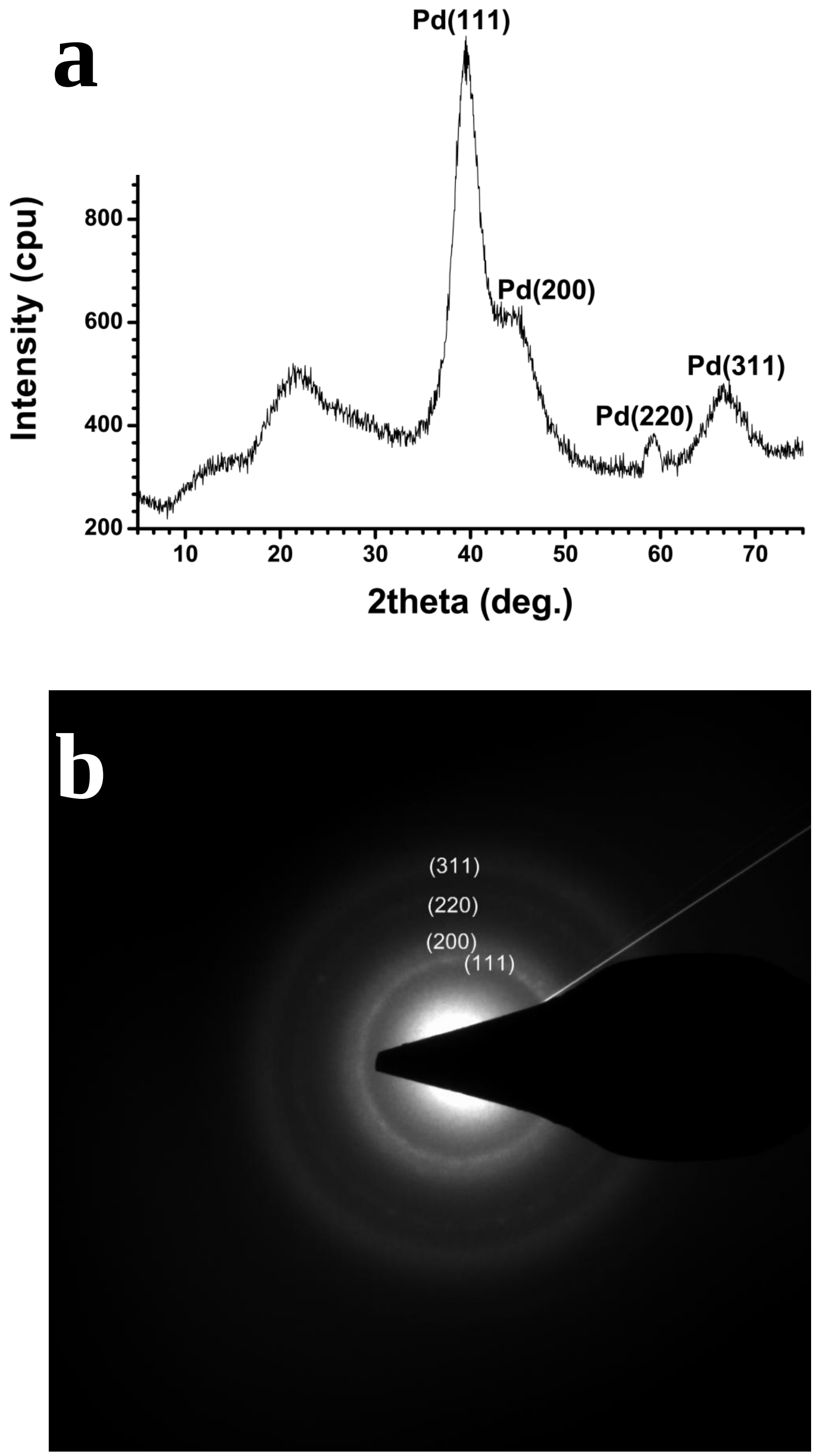

Figure 16. (a) Powder-XRD pattern (b) selected area electron diffraction image of PVP-stabilized palladium(0) nanoclusters.

“Figure 16a shows the powder-XRD patterns for the PVP-stabilized palladium(0) nanoclusters sample. The peak broadening is characteristic of the materials having nanometer particle size [95]. Four reflections are observed in the XRD pattern at 2θ of 39.5, 45, 59 and 66.5° that could be attributed to 111, 200, 220 and 311 peaks of elemental palladium[96], but another peak observed at 21.5° most probably belongs to the residual ammonium tetramethoxyborate species remaining on the surface of nanoclusters. These four reflections are also seen from the SAED image shown in Figure 16b indicating the presence of palladium in cubic structure” [59].

“^{11}B-NMR spectra taken from the reaction solution after the complete methanolysis of AB catalyzed by PVP-stabilized palladium(0) nanoclusters shows a single intense peak at $\delta \approx 8.6$ ppm which is readily assigned to the tetramethoxyborate $[B(OCH_3)_4]^-$ anion” [12, 59].

5.2. Kinetics of the Methanolysis of Ammonia-Borane Catalyzed by In-Situ Generated PVP-Stabilized Palladium(0) Nanoclusters

“As the first control test before starting the kinetic studies, the methanolysis of AB was performed in the absence of catalyst. In these test experiments performed at various temperature in the range of 15-35 °C, no detectable hydrogen gas evolution was observed from the self-methanolysis of AB over a period of 24 hours” [59].

“The in-situ generated PVP-stabilized palladium(0) nanoclusters are found to be highly active catalyst for the methanolysis of AB at low concentrations and room temperature. Figure 17 shows the plots of the volume of hydrogen generated versus time during the catalytic methanolysis of 200 mM H_3NBH_3 solution in the presence of palladium(0) nanoclusters in different Pd concentrations (0.50, 0.75, 1.00, 1.25, and 1.50 mM) at 25 ± 0.5 ^{o}C” [59].

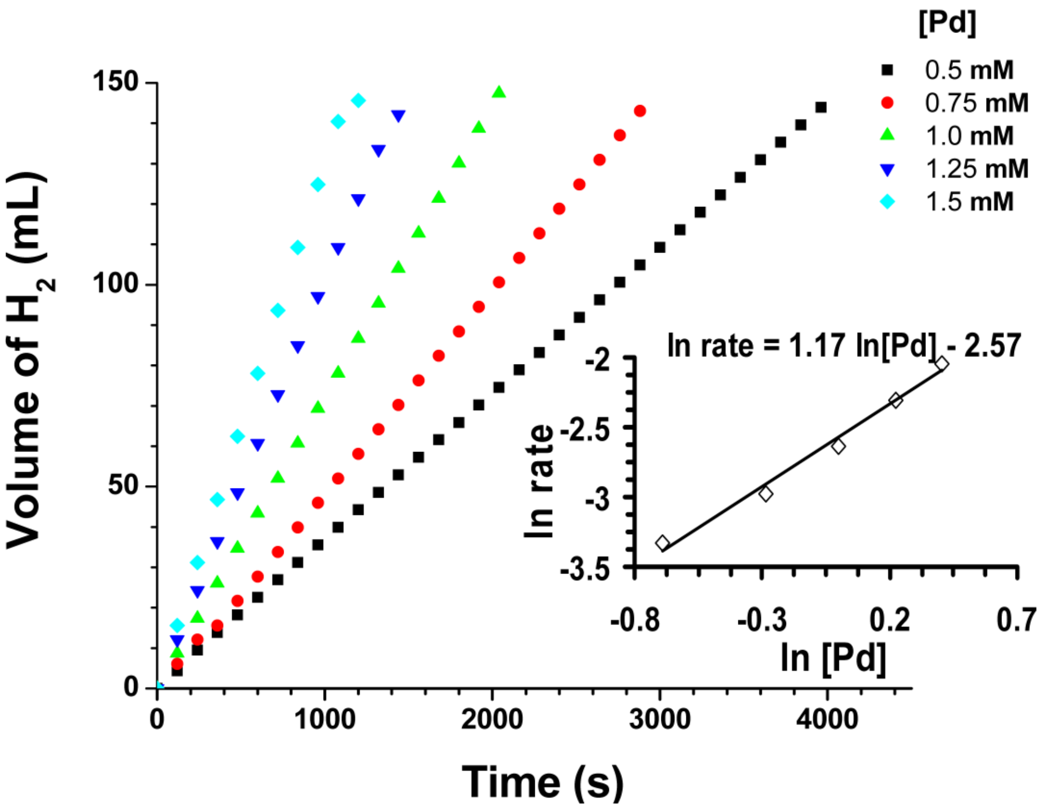

Figure 17. The volume of hydrogen versus time plot for the methanolysis of ammonia-borane catalyzed by PVP-stabilized palladium(0) nanoclusters depending on the palladium concentration. The inset shows the plot of hydrogen generation rate versus the concentration of palladium (both in logarithmic scale) at 25 ± 0.5 ^{0}C.

“The hydrogen generation rate was determined from the linear portion of the plot for each experiment. The plot of hydrogen generation rate versus palladium concentration, both in logarithmic scale (the inset in Figure 17) gives a straight line with a slope of 1.17 ≈ 1, indicating that the methanolysis reaction is first order with respect to the catalyst concentration” [59].

“The effect of AB concentration on the hydrogen generation rate was also studied by performing a series of experiments starting with various initial concentrations of H_3NBH_3 while keeping the catalyst concentration constant at 0.5 mM Pd. Figure 18 shows plots of the volume of hydrogen generated versus time during the catalytic methanolysis of AB at various AB concentrations” [59].

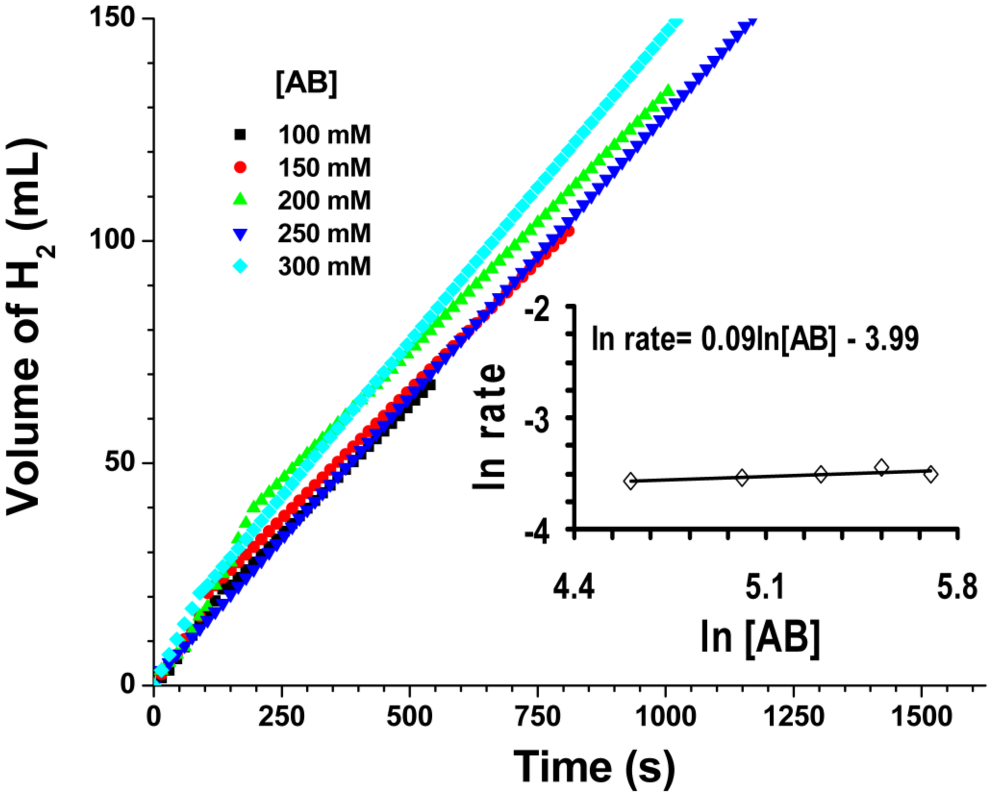

Figure 18. The volume of hydrogen versus time plots depending on the substrate concentrations at constant catalyst concentration (0.5mM) and the inset shows the plot of hydrogen generation rate versus the substrate concentration (both in logarithmic scale) at 25 ± 0.5 °C.

“The hydrogen generation rate was determined from the linear portion of the plot for each ammonia-borane concentration in the unit of ml H_2.min^{-1} and used for constructing the plot of hydrogen generation rate versus AB concentration, both in logarithmic scale (the inset in Figure 18). The slope of the line given in the inset of Figure 18 is 0.09 ≈ 0 indicating that the methanolysis reaction is zero order with respect to the ammonia-borane concentration. Ramachandran and Gagare was proposed similar kinetics in AB concentration for methanolysis of AB in the presence of $NiCl_2$ and $PdCl_2$ catalysts [12]” [59].

“Consequently, the rate law for the catalytic methanolysis of AB catalyzed by in-situ generated PVP-stabilized palladium(0) nanoclusters can be given as in Equation 5” [59].

$$\frac{-3d[H_3NBH_3]}{dt} = \frac{d[H_2]}{dt} = k[Pd] \tag{5}$$

“PVP-stabilized palladium(0) nanoclusters catalyzed methanolysis of AB was carried out at different temperature in the range of 15-35 °C starting with an initial substrate concentration of 200 mM H_3NBH_3 and a catalyst concentration of 1.0 mM Pd (Figure 19) in order to determine activation parameters of the reaction. The values of rate constants k (Table-1) for the methanolysis of AB catalyzed by PVP-stabilized palladium(0) nanoclusters were calculated from the slope of the linear part of each plot in Figure 19 and used to calculate the activation parameters” [59].

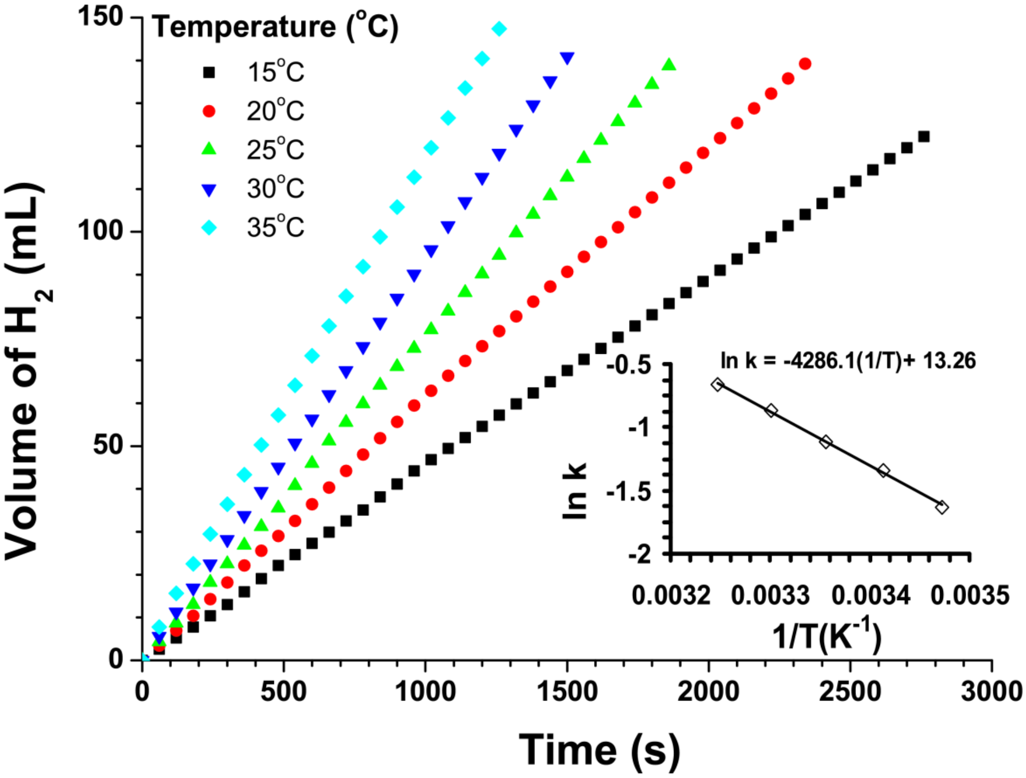

Figure 19. The volume of hydrogen versus time plots at different temperatures for the methanolysis of ammonia-borane catalyzed by PVP-stabilized palladium(0) nanoclusters in the temperature range 15-35 ^{o}C. The inset shows Arrhenius plot (ln k versus the reciprocal absolute temperature 1/T (K^{-1})).

Table 1. The values of rate constant k for the catalytic methanolysis of AB starting with a solution of 200 mM H_3NBH_3 and in-situ generated PVP-stabilized palladium(0) nanoclusters (1.0 mM Pd) at different temperatures calculated from hydrogen volume versus time.

Temperature (°C)	Rate Constant, k, (mol H_2.(mol Pd)$^{-1}$.s^{-1})
15	**0.195**
20	**0.261**
25	**0.326**
30	**0.419**
35	**0.516**

First, the Arrhenius equation was used for the calculating Ea:

$$k = A.e^{-\frac{Ea}{RT}} \qquad (6)$$

Where A and Ea are constants characteristics of the reaction and R is the gas constant [97]. Ea is the Arrhenius activation energy and A is the preexponential factor. The natural logarithm of Arrhenius equation gives us;

$$\mathrm{lnk} = \mathrm{lnA} - \left(\frac{\mathrm{Ea}}{\mathrm{RT}} \right) \tag{7}$$

The activation energy, E_a, of the methanolysis of AB catalyzed by PVP-stabilized palladium(0) nanoclusters was calculated from the slope of Arrhenius plot (inset of Figure 19). It was found as 35 ± 2 kJ·mol^{-1}. Secondly, The enthalpy of activation, $\Delta H^{\#}$ and the entropy of activation, $\Delta S^{\#}$ were calculated from the Eyring equation (Eq.8) by plotting the graph of $\ln \frac{k}{T}$ versus $\frac{1}{T}$ (Figure 20). From the slope and intercept of Figure 20, $\Delta H^{\#}$ was calculated as 33 ± 2 kJ·mol^{-1}and $\Delta S^{\#}$ was found as -150 ± 3 J·K^{-1}·mol^{-1}respectively.

$$\ln \frac{\mathrm{k}}{\mathrm{T}} = \frac{1}{\mathrm{T}} \left(\frac{-\Delta \mathrm{H}^{*}}{\mathrm{R}} \right) + \ln \frac{\mathrm{k_b}}{\mathrm{h}} + \frac{\Delta \mathrm{S}^{*}}{\mathrm{R}} \tag{8}$$

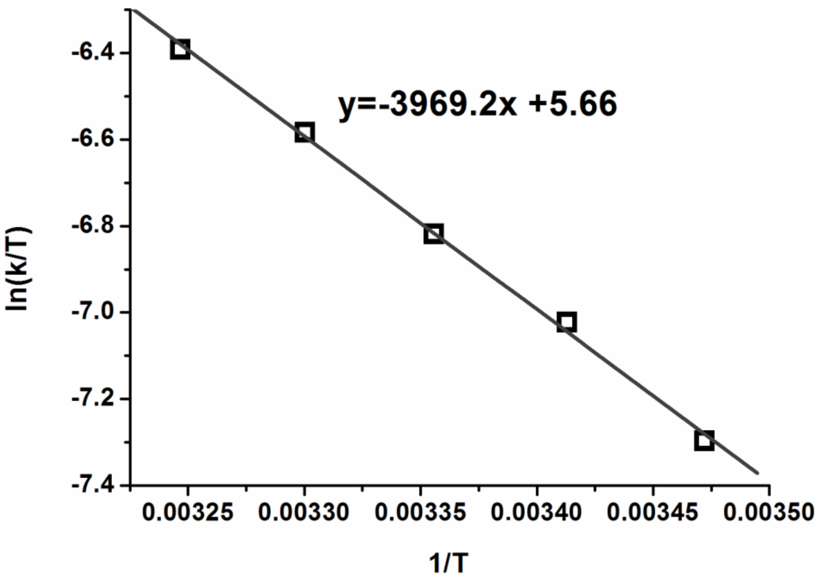

Figure 20. Eyring plot (ln(k/T) vs. 1/T(K^{-1})) for the PVP-stabilized palladium(0) nanoclusters catalyzed methanolysis of ammonia borane.

5.3. The Catalytic Lifetime of PVP-Stabilized Palladium0) Nanoclusters in the Methanolysis of Ammonia-Borane

“A catalyst lifetime experiment was performed starting with a 20 mL solution of PVP-stabilized palladium(0) nanoclusters containing 0.5 mM Pd and 0.5 M H_3NBH_3 plus 5 equiv. PVP at 25.0 ± 0.5 °C. The in-situ generated PVP-stabilized palladium(0) nanoclusters provide 23000 turnovers in the methanolysis of ammonia-borane over 27 hours before deactivation at 25.0 ± 0.5 °C. This makes them long-lived catalyst in the methanolysis of AB (Figure 21). It is noteworthy that this is the first total turnover number reported for the catalytic methanolysis of AB” [59].

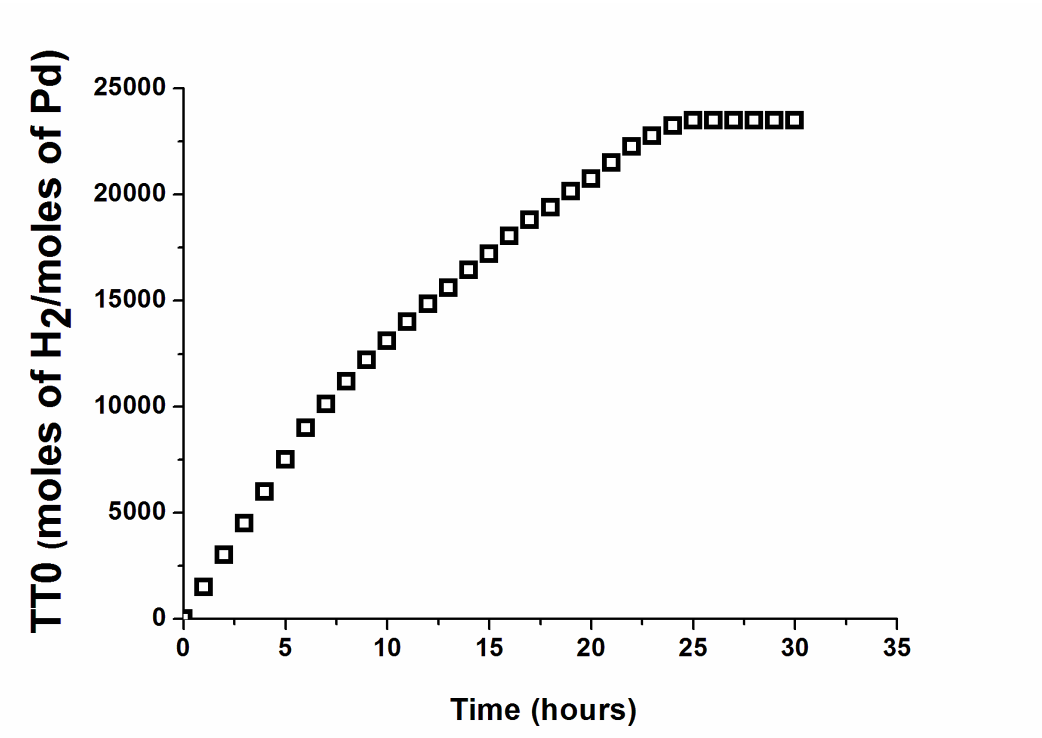

Figure 21. Plot of total turnover number (TTO) versus time for the methanolysis of AB catalyzed by PVP-stabilized palladium(0) nanoclusters at 25.0 ± 0.5 °C .

5.4. Mercury Poisoning

“The ability of Hg(0) to poison heterogeneous metal(0) catalysts [98], by amalgamating the metal catalyst or being adsorbed on its surface, has been known for a long time. The Hg(0)-poisoning experiment is easy to perform, but it is not definitive by itself nor universally applicable [99]. The suppression of catalysis by Hg(0) is considered as a compelling evidence for heterogeneous catalyst. After about 40% of conversion in a typical methanolysis experiment at 25.0 ± 0.5 °C, 300 equivalents of mercury per palladium was added into the reaction solution and the progress of reaction was followed by monitoring the H_2 volume, as shown in Figure 22. The cease of the catalytic methanolysis of AB completely upon mercury addition is a compelling evidence that Pd(0) nanoclusters are the true catalysis in the methanolysis of AB” [59].

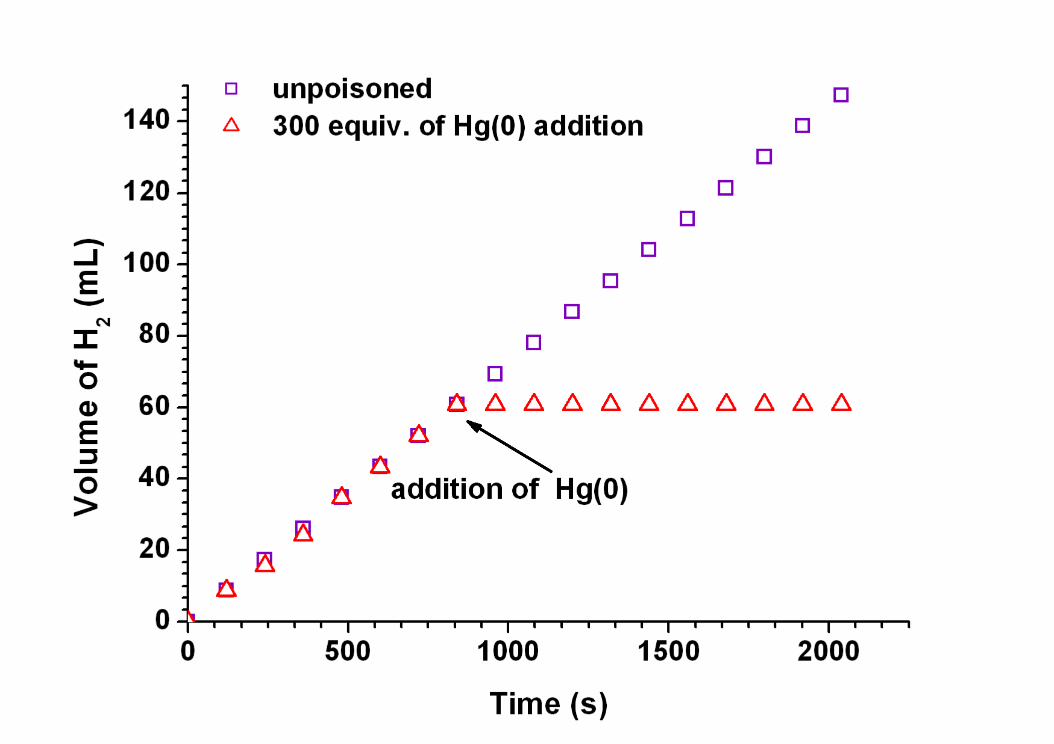

Figure 22. The volume of hydrogen versus time plots for catalytic methanolysis of 200 mM AB with and without addition of 300 equiv. Hg(0) at 25 ± 0.5 °C.

5.5. In-situ Generation and Characterization of PVP-Stabilized Ruthenium(0) Nanoclusters

Water soluble polymer stabilized ruthenium(0) nanoclusters were formed in situ from the reduction of ruthenium(III) chloride in the presence of PVP during the methanolysis of AB. In our protocol, PVP was used as a stabilizer and AB acted both reducing agent and substrate [23]. The observation of rapid color change from dark yellow to dark brown and concomitant hydrogen generation after addition of AB into the metal-polymer mixture indicate the formation of PVP stabilized ruthenium(0) nanoclusters. The reduction of Ru(III) to Ru(0) in the presence of PVP upon addition of AB was followed by UV-visible spectroscopy. Figure 23 shows the UV-Vis electronic absorption spectra of the methanol solution of Ru(III) chloride before and after addition of AB.

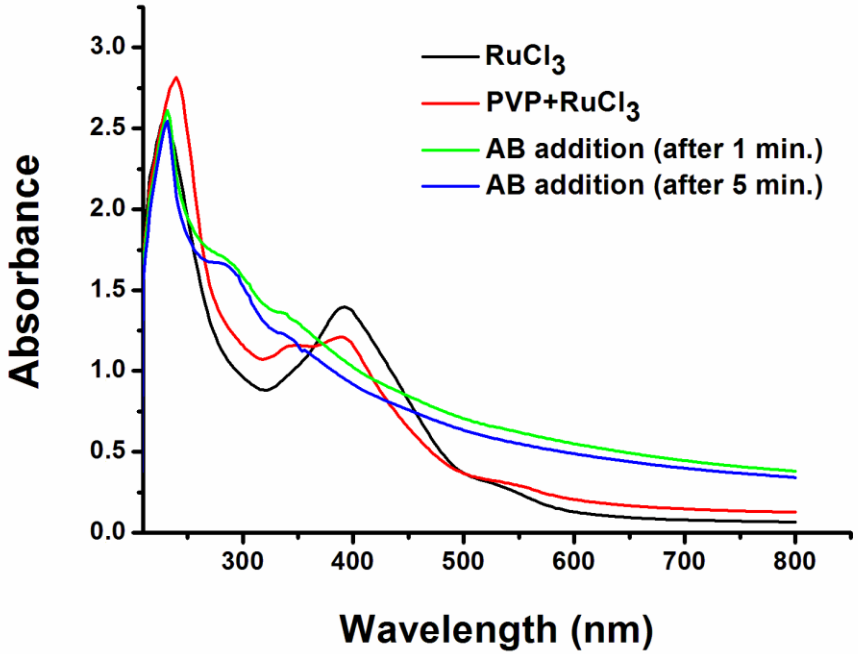

Figure 23. UV-Visible spectra of ruthenium (III) chloride, ruthenium (III) chloride plus PVP and PVP-stabilized ruthenium(0) nanoclusters taken from the methanol solution.

The disappearance of the d-d absorption peak at 390 nm of the ruthenium(III) chloride within one minute and the increasing absorption continua indicate the complete reduction of Ru(III) to Ru(0) and the formation of PVP-stabilized ruthenium(0) nanoclusters [32].

Many experiments performed at different polymer concentrations by keeping the metal concentration constant to find the optimum polymer to metal ratio. Results indicate that the highest stability and catalytic activity were obtained at PVP/Ru ratio of 20 for the PVP stabilized ruthenium(0) nanoclusters. The PVP-stabilized ruthenium(0) nanoclusters are highly stable in solution, even for months, and they can be isolated from the solution as solid materials by removing the volatiles in vacuum. The isolated PVP stabilized ruthenium(0) nanoclusters are also stable for months under inert atmosphere and they are readily redispersible in methanol by preserving their catalytic activity in the methanolysis of AB.

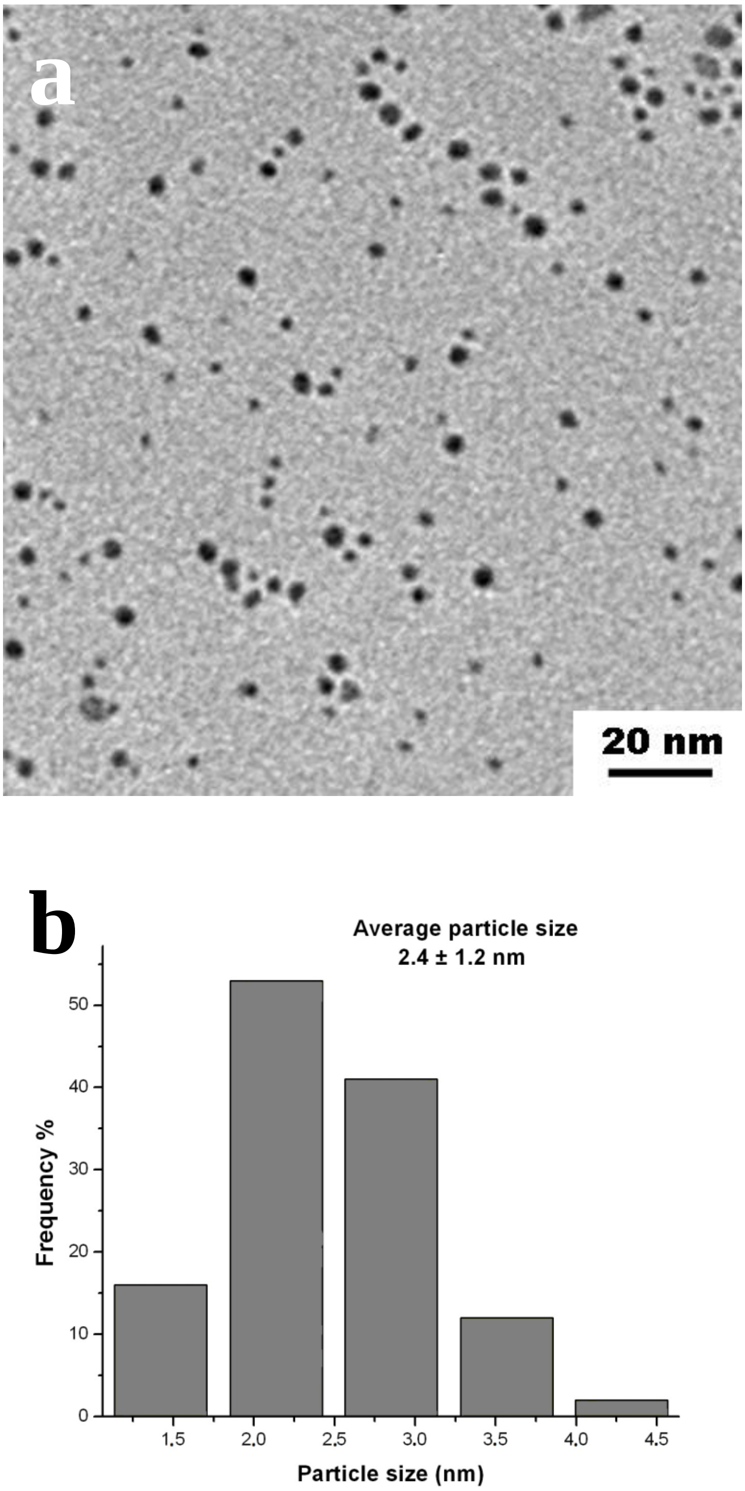

Figure 24. a) TEM images of PVP- stabilized ruthenium(0) nanoclusters b) corresponding particle size histogram.

Figure 24 shows the TEM image and corresponding particle size histogram of PVP-stabilized ruthenium(0) nanoclusters. From the TEM image we can conclude that PVP-stabilized ruthenium(0) nanoclusters are in spherical shape with an average particle size of 2.4 ± 1.2nm. It is also noteworthy that in situ generated PVP-stabilized ruthenium(0) nanoclusters during the methanolysis of AB are very stable and dispersive in solution while the nanoparticles previously used as catalysts in the methanolysis of AB have been shown to undergo rapid agglomeration. This stability lead to the nanoclusters being an effective and long live catalyst.

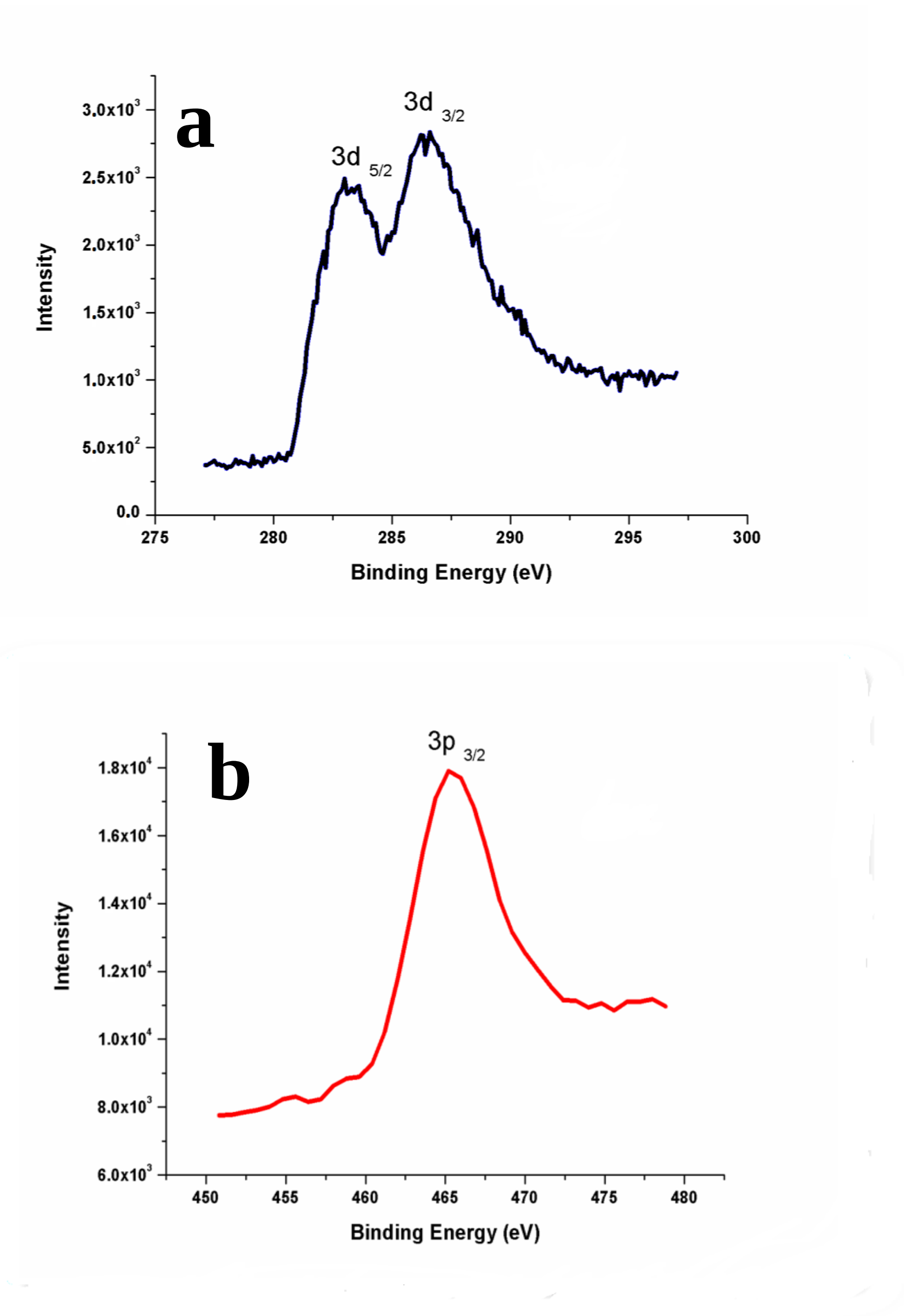

Figure 25. a) 3d region and b) 3p region in the X-Ray photoelectron spectrum of PVP-stabilized ruthenium(0) nanoclusters isolated from the reduction of ruthenium(III) chloride (1.5mM) by ammonia-borane (200 mM) in the presence of PVP.

Figure 25a and 25b show the XPS spectrum of PVP- stabilized ruthenium(0) nanoclusters. First spectrum (Figure 25a), shows two well resolved peaks at 283.8 and 288.1 eV, readily assigned to the Ru(0) $3d_{5/2}$ and Ru(0) $3d_{3/2}$, respectively, by comparing to the values of metallic ruthenium. In the second spectrum (Figure 25b) one prominent signal was observed at 462 eV for Ru 3p3/2. These signals are readily assigned to the Ru(0) [100].That no higher oxidation peaks are due to the highly protection of ruthenium(0) nanoclusters by PVP.

Figure 26 shows the X-ray diffraction pattern of the in situ generated PVP stabilized of ruthenium(0) nanoclusters.

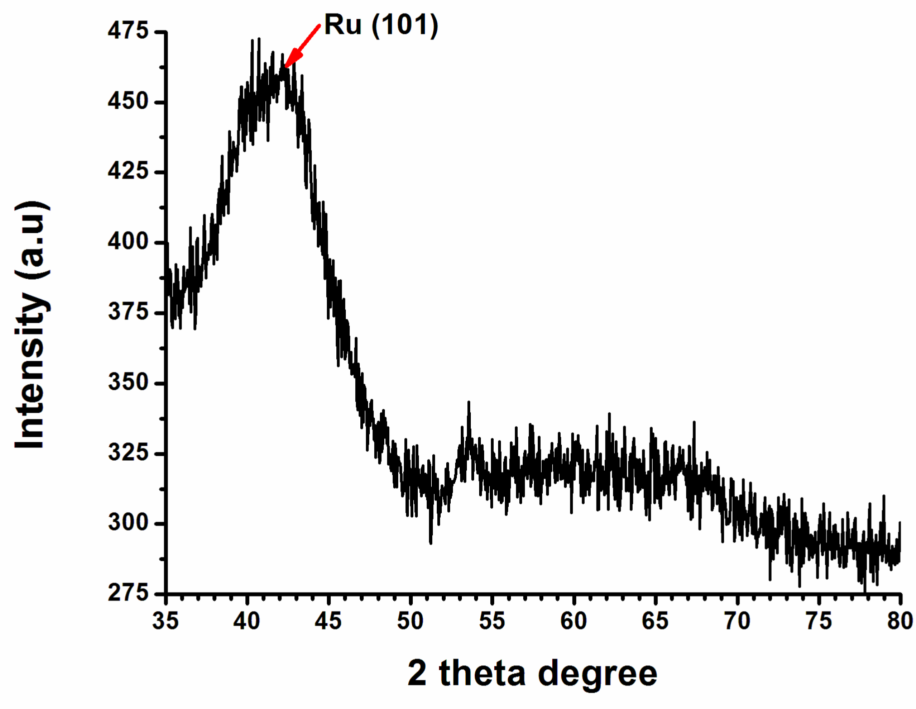

Figure 26. Powder X-ray diffraction pattern of in-situ generated PVP stabilized Ru(0) nanoclusters.

The most intense peak observed at $2\theta = 44^{\circ}$ belongs to Ru(101) plane [101]. A broadening observed at this plane is characteristic of materials having a nanometer particle size [95]. A particle size of 2.5 nm was calculated from the Scherrer formula almost matches with the average particle size of 2.4 nm calculated from the TEM image.

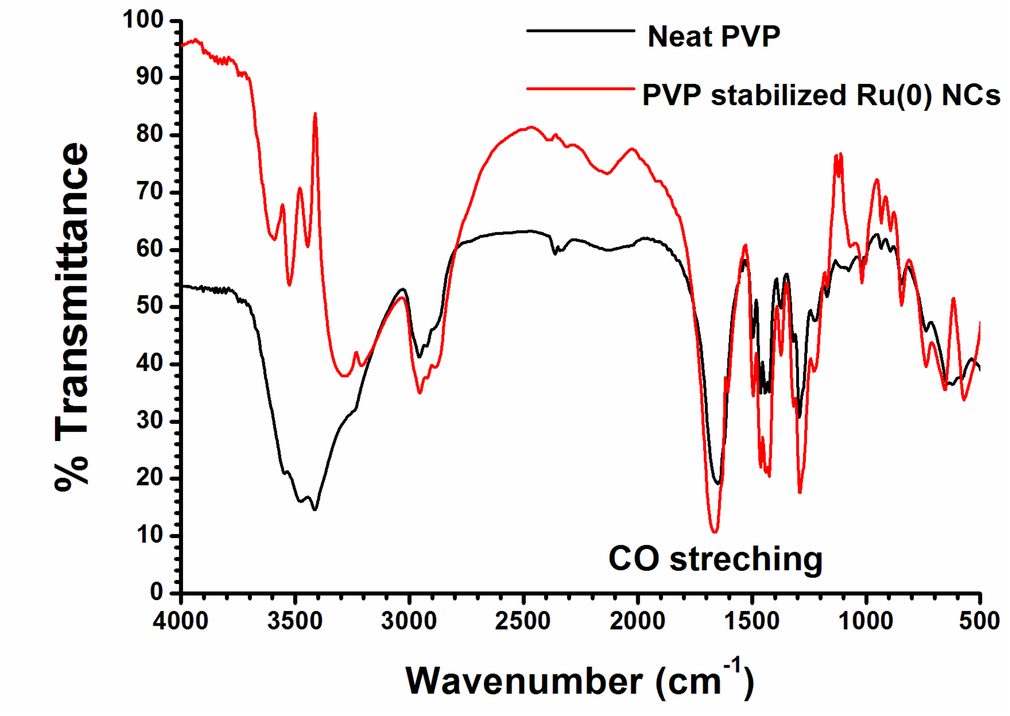

Figure 27. FT-IR spectra of the PVP-stabilized Ru(0) nanoclusters and neat PVP. The PVP-stabilized Ru(0) nanoclusters were isolated from the reduction of ruthenium(III) chloride (1.5 mM) by AB (200 mM) in the presence of PVP(30 mM).

Figure 27 reveals the FT-IR spectrum of the PVP-stabilized ruthenium(0) nanoclusters and neat PVP, taken from KBr pellet. Spectrum indicates the existence of PVP in the nanoclusters sample, most probably both for adsorbed on the surface of nanoclusters and for free PVP molecules due to the higher amount of PVP is needed to stabilize ruthenium(0) nanoclusters.

The ^{11}B-NMR spectra of the sample were taken from solution of the catalytic methanolysis of AB catalyzed by PVP stabilized ruthenium(0) nanoclusters. In the spectra, single intense peak was observed at $\delta \approx 8.6$ ppm which is readily assigned to the tetramethoxyborate $[B(OCH_3)_4]^-$ anion.

5.6. The Catalytic Activity of PVP-Stabilized Ruthenium(0) Nanoclusters in the Methanolysis of AB

The in situ-generated PVP-stabilized ruthenium(0) nanoclusters are found to be highly active catalysts for the methanolysis of AB even at low concentrations and room temperature. Figure 28 shows the plots of the volume of hydrogen generated versus time during the catalytic methanolysis of 200 mM H_3NBH_3 solution at different Ru concentrations (0.50, 1.00, 1.50, 2.00, and 2.50 mM) at $25 \pm 0.5\ ^{\circ}C$.

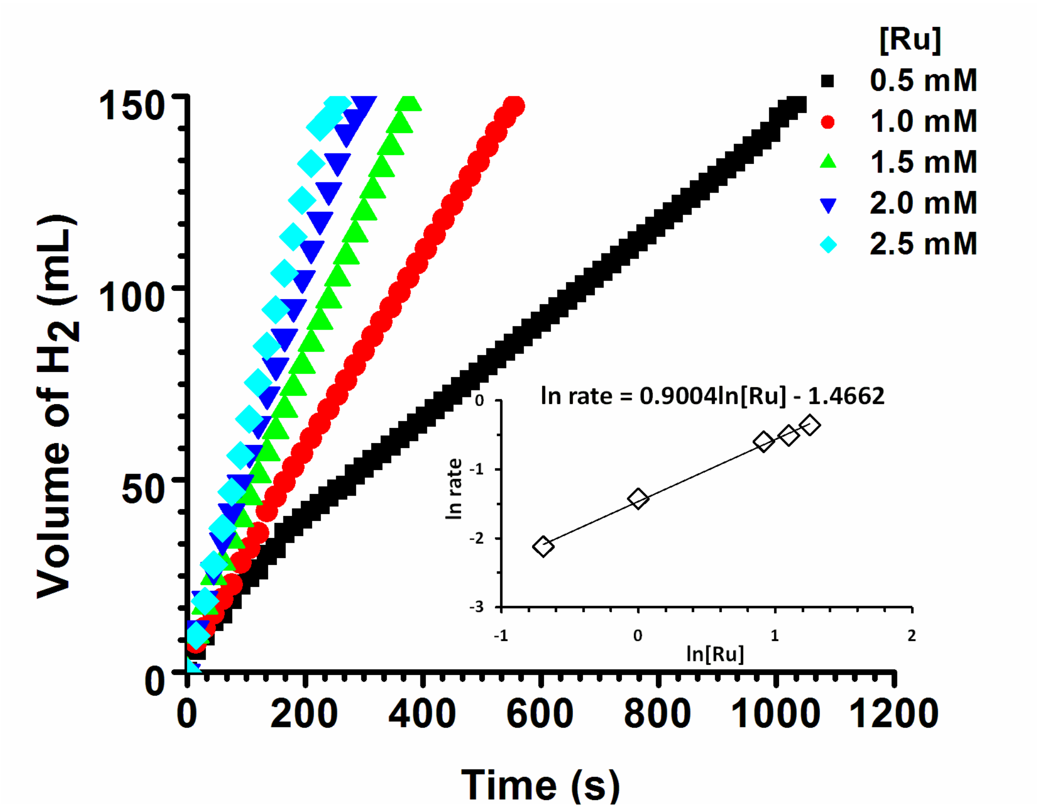

Figure 28. The volume of hydrogen versus time plots depending on the metal concentrations for PVP-stabilized ruthenium(0) nanoclusters at 25 ± 0.5 °C. The inset of figure shows the plot of hydrogen generation rate versus the concentration of ruthenium (both in logarithmic scale).

The plot of hydrogen generation rate versus Ru concentration, both in logarithmic scale (the inset in Figure 28), gives a straight line with a slope of 0.9004≈1, indicating that the methanolysis reaction is first order with respect to the catalyst concentration.

The effect of AB concentration on the hydrogen generation rate was also studied by performing a series of experiments starting with various initial concentrations of H_3NBH_3 while keeping the catalyst concentration constant at 1.5 mM. Figure 29a and Figure 29b shows plots of the volume of hydrogen generated versus time during the catalytic methanolysis of AB at various substrate concentrations.

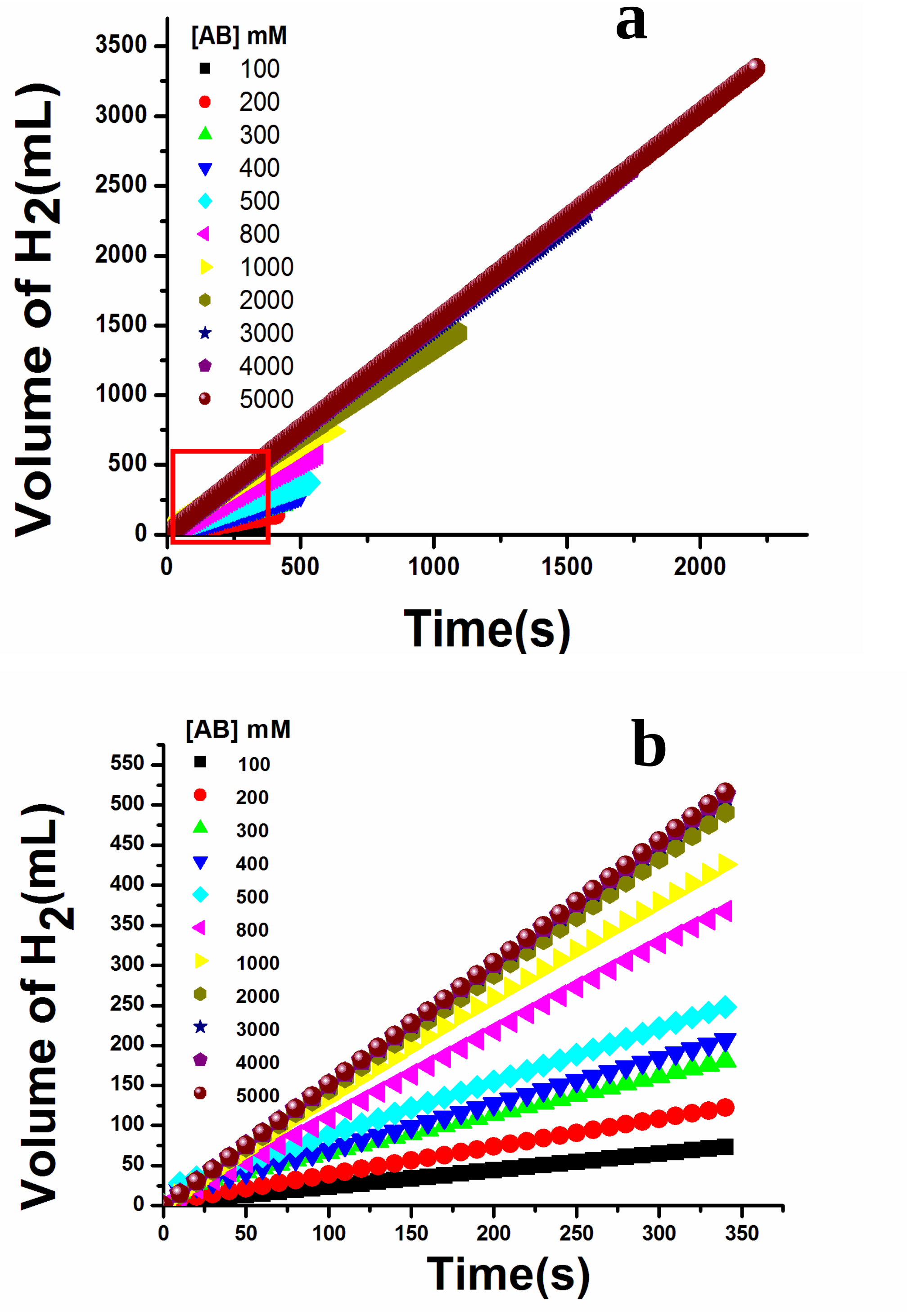

Figure 29. (a) The volume of hydrogen versus time plots depending on AB concentrations for PVP-stabilized ruthenium(0) nanoclusters at 25 ± 0.5 °C.(b) High magnified red rectangular region.

The hydrogen generation rate (mL H_2.min^{-1}) was determined from the linear portion of the plot for each ammonia–borane concentration and used for constructing the plot of hydrogen generation rate versus AB concentration in logarithmic scale (Figure 30).

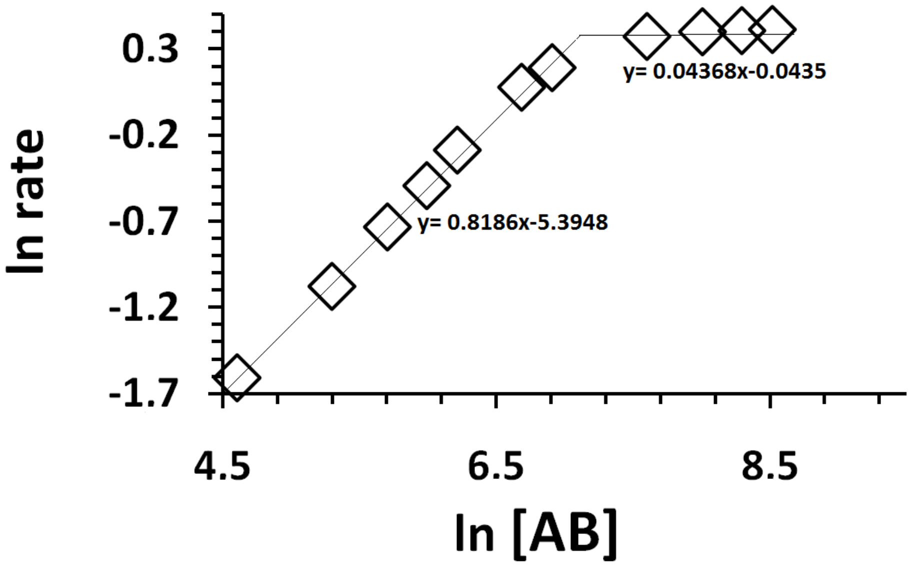

Figure 30. The logarithmic scale plot of hydrogen generation rate versus concentration of AB catalyzed by PVP-stabilized Ru(0) nanoclusters.

The slope of the line in the first part of the plot given in Figure 30 is 0.8186≈1, but the slope of the line in the second part is 0.0436≈0. This result indicates that when pseudo first order conditions are established, ([AB]>>[Ru]) in this case after [AB]/[Ru]=1333, the reaction rate law becomes zero order with respect to [AB]. Consequently, the rate law for the catalytic methanolysis of AB catalyzed by in situ generated PVP-stabilized ruthenium(0) nanoclusters can be given as in Equation 9;

$$-3d[H_3NBH_3] / dt = d[H_2] / dt = k[Ru] \qquad (9)$$

In order to determine activation parameters of the reaction, methanolysis of AB catalyzed by PVP-stabilized ruthenium(0) nanoclusters was carried out at different temperatures in the range of 15–35 °C (Figure 31), starting with an initial substrate concentration of 200 mM H_3NBH_3 and a catalyst concentration of 1.5 mM Ru.

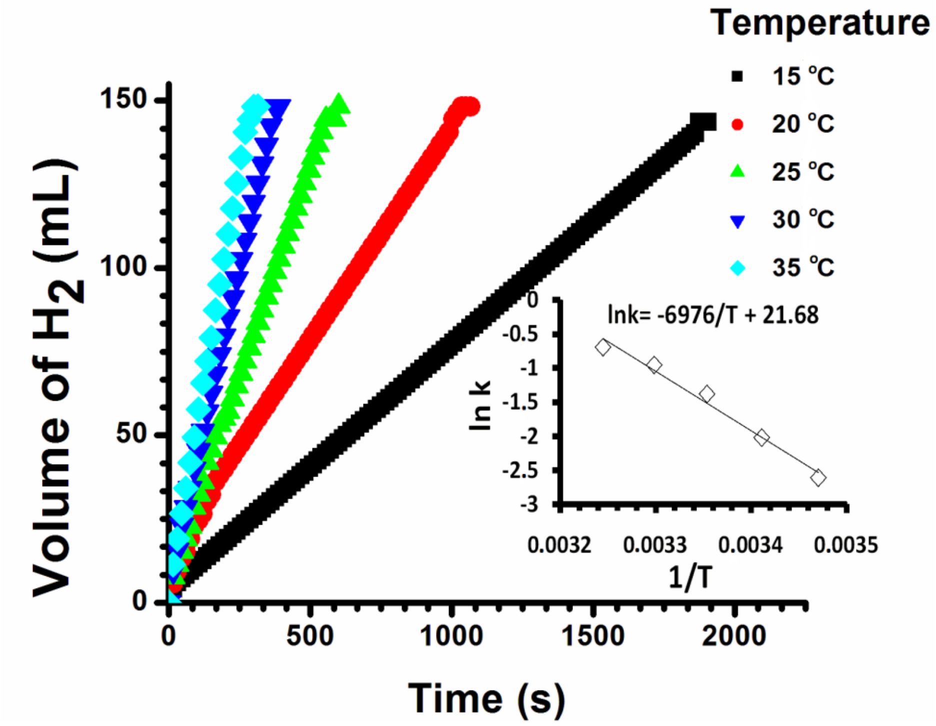

Figure 31. Volume of hydrogen versus time plot at different temperatures for the hydrolysis of AB (200 mM) catalyzed by PVP-stabilized ruthenium(0) nanoclusters (1.5 mM) in the temperature range 15-35 °C. The insets of the figure shows Arrhenius plot (ln k versus the reciprocal absolute temperature 1/T (K^{-1})).

The values of rate constants, k (Table-2), were calculated from the slope of the linear part of each plot in Figure 30 and used to draw Arrhenius plot (inset of Figure 31) and Eyring plot (Figure 32).

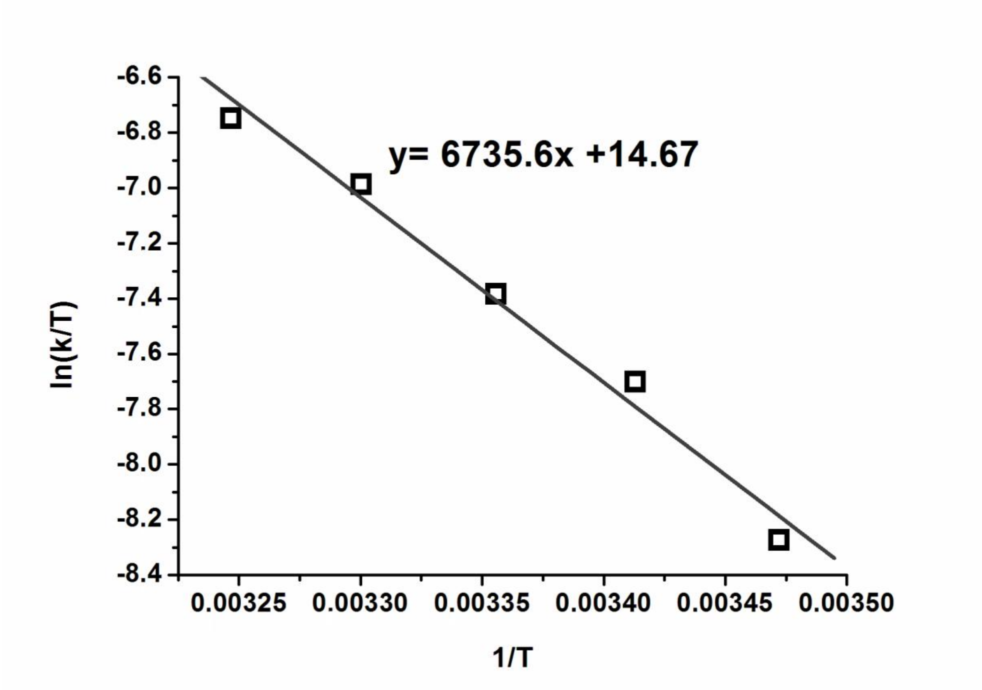

Figure 32. Eyring plot (ln(k/T) vs 1/T(K^{-1}) for the PVP-stabilized ruthenium(0) nanoclusters catalyzed methanolysis of ammonia borane.

From those graphs activation parameters were calculated as: Arrhenius activation energy, Ea = 58 ± 2 kJ mol^{-1}; activation enthalpy, $\Delta H^{\neq}$ = 56 ± 2 kJ mol^{-1}; activation entropy, $\Delta S^{\neq}$ = -75 ± 3 J K^{-1} mol^{-1}.

Table 2. The values of rate constant k for the catalytic methanolysis of AB starting with a solution of 200 mM H_3NBH_3 and in-situ generated PVP-stabilized ruthenium(0) nanoclusters (1.5 mM Ru) at different temperatures calculated from hydrogen volume versus time.

Temperature (°C)	**Rate Constant, k, (**mol H_2.(mol Ru)$^{-1}$.(molAB)$^{-1}$.s^{-1})
15	0.0734
20	0.1324
25	0.185
30	0.2757
35	0.361

5.7. The Catalytic Life Time of PVP-Stabilized Ruthenium(0) Nanoclusters in the Methanolysis of AB

A catalyst lifetime experiment was performed starting with a 20 mL solution of PVP-stabilized ruthenium(0) nanoclusters containing 0.125 mM Ru and 200 mM H_3NBH_3 at 25.0 ± 0.5 °C. The in situ-generated PVP-stabilized Ru(0) nanoclusters are long-lived catalysts providing 71500 turnovers in the methanolysis of AB over 25 h before deactivation (Figure 33).

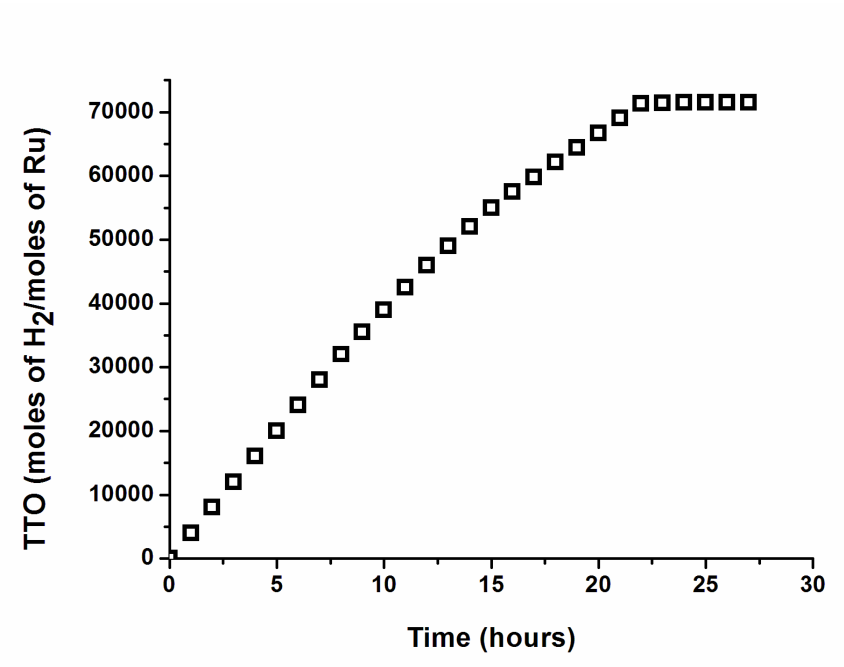

Figure 33. Plot of total turnover number (TTO) versus time for the methanolysis of AB catalyzed by PVP-stabilized ruthenium(0) nanoclusters at 25.0 ± 0.5 °C .

The average TOF value was found as 2860 h^{-1}. It is noteworthy that this is the first total turnover number and turnover frequency reported for a ruthenium catalyst in the catalytic methanolysis of AB.

5.8. Heterogeneity Test of PVP-Stabilized Ruthenium(0) Nanoclusters in the Methanolysis of AB

It has been known for a long time that Hg(0) has an ability to poison heterogeneous metal(0) catalysts [35] by amalgamating the metal catalyst or being adsorbed on its surface. The suppression of catalysis by Hg(0) is considered as evidence for heterogeneous catalysis. After about 40% of conversion in a typical methanolysis experiment, 350 equivalents of mercury per ruthenium was added into the reaction solution and the progress of reaction was followed by monitoring the H_2 volume, as shown in Figure 34.

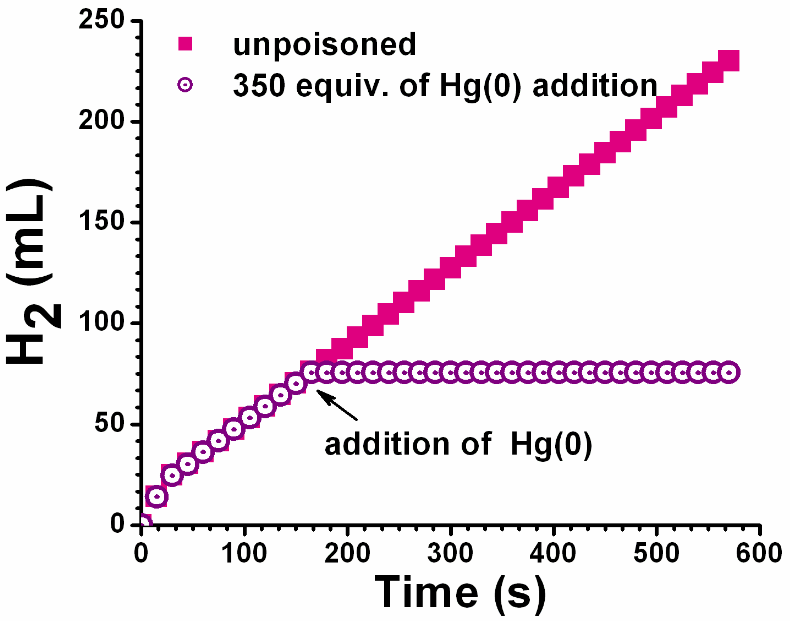

Figure 34. The volume of hydrogen versus time plots for catalytic methanolysis of 400 mM AB with and without addition of 350 equiv. Hg(0) at 25 ± 0.5 ºC.

The complete cessation of the catalytic methanolysis of AB upon mercury addition is additional evidence that ruthenium(0) nanoclusters are the true heterogenous catalyst in the methanolysis of AB.

CHAPTER 6

CONCLUSIONS

AB has been considered as an effective hydrogen storage material and methanolysis of AB attracts much attention in terms of recyclability of the reaction product and no ammonia liberation in the reaction.

In this thesis we have shown that in-situ generated PVP-stabilized palladium(0) and ruthenium(0) nanoclusters are highly active catalysts in the methanolysis of ammonia-borane.

“PVP-stabilized palladium(0) nanoclusters were easily generated in-situ during the methanolysis of ammonia-borane from the reduction of a commercially available precursor. The PVP stabilizer can provide enough stabilization for the palladium(0) nanoclusters so that they are very stable in solution under inert atmosphere and yet highly active catalysts for hydrogen generation from the methanolysis of ammonia-borane at room temperature. PVP-stabilized palladium(0) nanoclusters could be isolated as stable solid materials and well characterized. PVP appears to be a strongly stabilizing ligand for the palladium(0) nanoclusters, providing relatively small size and narrow size distribution (3.2 ± 0.5 nm). Although a strong stabilizer such as PVP would sturdily control the nanocluster formation, the particle size is expected to be affected also by the experimental conditions such as temperature and concentrations (substrate, precursor, and stabilizer). Such a study was considered beyond the scope this paper. PVP-stabilized palladium(0) nanoclusters are isolable and re-dispersible. More importantly, when re-dispersed in methanol they retain their catalytic activity in the methanolysis of ammonia-borane. The kinetics of methanolysis of AB was reported for the first time on the reaction catalyzed by PVP-stabilized palladium(0) nanoclusters. PVP-stabilized palladium(0) nanoclusters are long-lived catalysts in the methanolysis of AB providing 23000 turnovers over 27 h before deactivation at room temperature. Easy preparation, high stability, and the high catalytic performance make the in-situ generated PVP-stabilized palladium(0) nanoclusters a promising catalyst candidate to be employed in developing highly efficient portable hydrogen generation systems using AB as solid hydrogen storage material. Although palladium metal is more expensive than the first row metals, the in-situ generated PVP-stabilized palladium(0) nanoclusters are highly active catalyst in hydrogen generation from the methanolysis of AB even in low catalyst concentrations at room temperature. This can make palladium(0) nanoclusters as attractive catalyst" [59].

In the same way, PVP-stabilized ruthenium(0) nanoclusters were easily generated in situ and were successfully employed as catalyst in the methanolysis of AB. The reduction of ruthenium(III) chloride by AB in the presence of PVP yields nearly spherical and very stable ruthenium(0) nanoclusters with an average particle size of 2.4 nm. The PVP was employed as a stabilizer thus the ruthenium(0) nanoclusters are stable in solution under inert atmosphere and yet highly active catalysts for hydrogen generation from the methanolysis of AB at room temperature. In situ generated PVP stabilized ruthenium(0) nanoclusters could be isolated as stable solid materials and they are readily redispersible in methanol by preserving their activity in the methanolysis of AB. Furthermore, PVP-stabilized ruthenium(0) nanoclusters are long-lived catalysts in the methanolysis of AB, providing 71500 turnovers over 25 h before deactivation at room temperature. The superb catalytic activity and long lifetime of the nanoclusters stem from their small size and well-dispersion in the reaction medium. Easy preparation, outstanding stability, and the effective catalytic performance make in situ-generated PVP-stabilized ruthenium(0) nanoclusters leading candidates to be employed in developing highly efficient portable hydrogen generation systems using AB as a solid hydrogen storage material.

When we compare the performance of in-situ generated PVP stabilized palladium(0) and ruthenium(0) nanoclusters as catalyst in the methanolysis of AB, ruthenium(0) nanoclusters (2.4 nm) show higher activity than palladium(0) nanoclusters (3.2 nm) owing to its smaller particle size and larger active surface area which can be concluded from the Hg(0) poisoning test. Ruthenium(0) nanoclusters are more stable catalyst than palladium(0) nanoclusters comparing the TTO value of the catalysts 71500 and 23000, respectively. At higher AB to catalyst ratio, they show similar kinetics which is first order with respect to catalyst concentration and zero order with respect to AB concentration. Moreover, the activation energy calculated for palladium(0) nanoclusters catalyzed methanolysis of AB is lower than one calculated for ruthenium(0) nanoclusters indicating the higher temperature dependence of ruthenium(0) nanoclusters.

REFERENCES

[1] Dowson J. K., Nature, **1974**, 249, 724.

[2] Vriesa B.J.M, Vuurenb D.P., Hoogwijk M.M., Energy Policy, **2007**, 35, 2590-2610.

[3] Siblerud R., Our Future Is Hydrogen: Energy, Environment, and Economy, New Science Publications, Wellington, USA, **2001**.

[4] Basic Research Needs for the Hydrogen Economy, Report of the Basic Energy Sciences Workshop on Hydrogen Production, Storage and Use, May 13-15, Office of Science, U. S. Department of Energy, **2003**.

[5] Schlapbach L., Züttel A., Nature, **2001**, 414, 353.

[6] Rosi N. L., Eckert J., Eddaoudi M., Vodak D. T., Kim J., O'Keeffe M., Science, **2003**, 300, 1127.

[7] Annual Energy Outlook 2005 With Projections to 2025, Energy Information Administration, February **2005**, www.eia.doe.gov/oiaf/aeo/pdf/0383(2005).pdf. Last visited 20/04/2010.

[8] Deluga G. A., Salge J. R., Schmidt L. D., Verykios X. E., Science, **2004**, 303, 993.

[9] Liu B.-H, Li Z.-P., J. Power Sources, **2009**, 187, 527.

[10] Schlesinger H. I., Brown H. C., Finholt A. B., Gilbreath J. R., Hockstra H. R., Hydo E. K., J. Am. Chem. Soc., **1953**, 75, 215.

[11] Hsueh C.L., Liu C.H., Chen B.H., Chen C.Y., Kuo Y.C., Hwang K.J., Ku J.-R., Int. J. Hydrogen Energy, **2009**, 34, 1717.

[12] Ramachandran P. V., Gagare P. D., Inorg. Chem., **2007**, 46, 7810.

[13] Wang J.S., Geanangel R. A., Inorg. Chim. Acta., **1988**, 148, 185.

[14] Stephens F. H., Baker R. T., Matus M. H., Grant D. J., Dixon D. A., Angew. Chem. Int. Ed., **2007**, 46, 746.

[15] Jaska C. A., Temple K., Lough A. J., Manners I., J. Am. Chem. Soc., **2003**, 125, 9424.

[16] Denney M. C., Pons V., Hebden T. J., Heinekey D. M., Goldberg K. I., J. Am. Chem. Soc., **2006**, 128, 12048.

[17] Keaton R. J., Blacquiere J. M., Baker R. T., J. Am. Chem. Soc., **2007**, 129, 1844.

[18].Umegaki T., Yan J.M., Zhang X.B., Shioyama H., Kuriyama N., Xu Q., Int. J. Hydrogen Energy, **2009**, 34, 2303.

[19] Storozhenko P. A., Svitsyn R. A., Ketsko V. A., Buryak A K., Ulyanov A. V., Russ. J. Inorg. Chem., **2005**, 50, 980.

[20] (a) Zahmakıran M., Özkar S., Applied Catal.B:Env., **2009,** 89, 104. (b) Metin Ö., Özkar S., Energy&Fuels, **2009**, 23, 3517.

[21] Kalidindi S. B., Sanyal U., Jagirdar B. R., Phys. Chem. Chem. Phys., **2008**, 10, 5870.

[22] Kalidindi S. B., Vernekar A. A., Jagirdar B. R., Phys. Chem. Chem. Phys., **2009**, 11, 770.

[23] Chandra M., Xu Q., J. Power Sources, **2007,** 168, 135.

[24] Özkar S., Zahmakıran M., Journal of Alloys and Compounds, **2005**, 404-406, 728-731.

[25] Turkevich J., Kim G., Hillier J., Discuss. Faraday Soc., **1951**, 11, 55-75.

[26] Evans D. F., Wennerström H., The Colloidal Domain, 2nd ed.; Wiley-VCH: New York, **1999**.

[27] Finke R.G., Özkar S., Coordination Chemistry Rewievs, **2004**, 248, 135-146.

[28] (a) Teranishi T., Miyake M., Chem. Mater., **1998**, 10, 594; (b) Li Y., Bone E., El-Sayed M.A., Langmuir**, 2002**, 18, 4921.

[29] Xiong R., Maclellan J.M., Chen J., Yin Y., Li Z.Y., Xia Y., J. Am. Chem. Soc., **2005**, 127, 17718.

[30] (a) Li D., Komarneni S., J.Nanosci. Nanotech., **2008**, 8, 3930. (b) Xu D., Barbosa S., Yeates S.G., Polym.Preprints, **2008**, 49, 915.

[31] (a) Hou W., Dehm N.A., Scott R.W.J., J.Catal., **2008,** 253, 22. (b) Wang Y., Du M., Xu J., Yang P., Du Y., J. Disp.Sci.Tech., **2008,** 29, 891. (c) Papp S., Dekany I., Colloid Poly.Sci., **2006**, 284, 1049.

[32] Zhang Y., Yu J., Niu H., Liu H., J. Colloid Interface Sci., **2007**,313, 503.

[33] Zawadzki M., Okal J., Mater. Res. Bull., **2008**,43,3111.

[34] Yang J., Lee J.Y., Deivaraj T.C., Too H-P., J. Colloid Interface Sci., **2004**, 271, 308.

[35] Whitesides G. M., Hackett M., Brainard R. L., Lavalleye J. P., Sowinski A. F., Izumi A. N., Moore S. S., Brown D. W., Staudt E. M., Organometallics, **1985**, 4, 1819.

[36] Song C., Catal. Today, **2006**, 115, 2-32.

[37] Weisz P.B., Phys. Today, **2004,** 57, 47–52.

[38] Melillo J.M., Mcguire A.D., Kicklighter D.W., Moore B., Vorosmarty C.J., Schloss A.L., Nature, **1993,** 363, 234–240.

[39] Song C.S., Schobert H.H., Fuel Process. Technol., **1993,** 34, 157–196.

[40] Stwertka A., A Guide to the Elements, Oxford University Press., pp. 16–21. **1996,** ISBN 0-19-508083-1.

[41] Winter M., "Hydrogen: historical information". WebElements Ltd. http://education.jlab.org/itselemental/ele001.html. Retrieved 05/02/**2008**.

[42] Danish Department of Energy. Energy 21 (plan scenario 1988 and follow up 1999). Copenhagen: Government Press.

[43] Penner S.S., Energy, **2006**, 31, 33–43

[44] (a) Bonner M., Botts T., McBreen J., Mezzina A., Salzano F., and Yang C., Int. J. Hydrogen Energy, **1984**, 9, 4, 269–275. (b) Dutta S., Technology, Int. J. Hydrogen Energy, **1990**, 15, 6, 379–386.

[45] Baykara S.Z., Bilgen E., International Journal of Hydrogen Energy, **1989**, 14, 12, 881–889.

[46] (a) Wendt H., Engels H., Int. J. Hydrogen Energy, **1987**, 12, 5, 291–295. (b) Yalcin S., Int. J. Hydrogen Energy, **1989,**14, 8, 551–561.

[47] (a) Bull S.R., Hydrogen Production by Photoprocesses, Proceedings International Renewabe Energy Conference, Honolulu, Hawaii, **1988**, 413–426. (b) Willner I., Steinberger-Willner B., Int. J. Hydrogen Energy, **1988**, 13, 10, 593–604.

[48] National Hydrogen Association, The Hydrogen Technology Assessment, Phase I, Report for NASA, Washington, DC, **1991.**

[49] Sherif S.A., Barbir F., Veziroglu T.N., The Electricity Journal, **2005**, 18, 6.

[50] Marbán G., Valdés-Solís T., Int. J. Hydrogen Energy, **2007**, 32, 1625 – 1637.

[51] Marrero-Alfonso E. Y., Beaird A. M., Davis T. A., Matthews M. A., Industrial & Engineering Chemistry Research, **2009**, 48, 3703–3712.

[52] Basic Research Needs For the Hydrogen Economy, Report of the Basic Energy Sciences Workshop on Hydrogen Production, Storage and Use, Office of Science, U.S. Department of Energy, May 13–15, **2003**.

[53] Grochala W., Edwards P. P., Chem. Rev., **2004**, 104, 1283.

[54] IAC Report, Lighting the Way Towards a Sustainable Energy Futures, Interacademy Council, Amsterdam, **2007**.

[55] (a) Marder T. B., Angew. Chem. Int. Ed., **2007**, 46, 8116. b) Stephens F. H., Pons V., Baker R. T., Dalton Trans., **2007**, 2613.

[56] (a) Amendola S.C., Janjua J.M., Spencer N.C., Kelly M.T., Petillo P.J., Sharp-Goldman S.L., Binder M., Int. J. Hydrogen Energy, **2000**, 25, 969-975. (b) Lee J.Y., Lee H.H., Lee J. H., Kim D.M., Kim J.H., J. Electrochem. Soc., **2002**, 149, 603-606.

[57] (a) Mohajeri N., Raissi A.T., Adebiyi O., Journal of Power Sources, **2007**,167 482. (b) Stowe A.C., Shaw W.J., Linehan J.C., Schmid B., Autrey T., Phys. Chem. Chem. Phys., **2007**, 9, 1831. (c) Stephens F.H., Baker R.T., Matus M.H., Daniel J., Dixon D.A., Angew.

Chem. Int. Ed., **2007**, 46 746. (d) Keaton R.J., Blacquiere J.M., Baker R.T., J. Am. Chem. Soc., **2007**, 129, 1844.

[58] (a) Clark T. J., Whittell G. R., Manners I., Inorg. Chem., **2007**, 46, 7522. (b) Cheng F., Ma H., Li Y., Chen J., Inorg. Chem., **2007**, 46, 788. (c) Chandra M., Xu Q., J. Power Sources, **2006**, 159, 855. (d) Chandra M., Xu Q., J. Power Sources, **2006**, 163, 364.

[59] Erdogan H., Metin O., Ozkar S., Phys. Chem. Chem. Phys., **2009**, 11, 10519-10525.

[60] Caliskan S., Zahmakiran M., Ozkar S., Applied Catalysis B: Environmental, **2010**, 93, 387-394.

[61] Klabunde K. J., Stark J., Koper C., Park D., J. Phys. Chem., **1996**, 100, 12142.

[62] Grassian V. H., J. Phys. Chem., **2008,** 112, 18303–18313.

[**63**] Aiken III J.D., Lin Y., Finke R.G., J. Mol. Catal. A, **1996,** 114, 29-5.

[**64**] Schmid G. (Ed), Clusters and Colloids: From Theory to Applications, VCH Publishers, New York, **1994.**

[65] Jongh L.J.(Ed), Physics and Chemistry of Metal Cluster Compounds, Kluwer Publishers, Dordrect, **1994.**

[66] Simon U., Schön G., Schmid G., Angew Chem. Int. Ed. Eng., **1990**, 248, 1186.

[67] Glanz J., Science, **1995**, 269, 1363.

[68] Antonietti M., Göltner C., Angew Chem. Int. Ed. Eng., **1997**, 36, 910.

[69] Elghanian R., Storhoff J.J., Mucic R.C., Setinger R.L., Mirkin C.A., Science, **1997**, 277, 1078.

[70] Colvin V.L., Schlamp M.C., Alivisatos A.P., Nature, **1994**, 370, 354.

[71] Sonti S.V., Bose A., J. Colloid Int. Sci., **1995**, 170, 575.

[72] Vossmeyer T., Delenno E., Heath J.R., Angew. Chem., Int. Ed. Eng., **1997**, 36, 1080.

[73] (a) Lin Y., Finke R. G., J. Am. Chem. Soc., **1994**, 116, 8335. (b) Bönneman H., Braun G.A., Angew Chem. Int. Ed. Eng., **1996**, 35, 1992. (c) Lewis L.N., Lewis N., J. Am. Chem. Soc., **1986**, 108, 7228. (d) Wilcoxon J.P., Martinho T., Klavetter E., Sylwester A.P., Nanophase Mater. **1994**,771. (e) Na Y., Park S., Bong S.H., J. Am. Chem. Soc., **2004**, 126, 250. (f) Pelzer K., Vidoni O., Phillot K., Chaudret B., Colliére V., Adv. Func. Mater., **2003**, 12, 118. (g) Hostetler M., Wingate J., Zong C., Evans N., Murray R., Langmuir, **1998**, 14, 17-30. (h) Pool R., Science, **1990,** 248, 1186-1188.

[74] Roucoux A., Schulz J., Patin H., Chem. Rev., **2002**, 102, 3757-3778.

[75] Tan C. K., Newberry V., Webb T. R., McAuliffe C. A., Dalton Trans. **1987**, 1299.

[76] Balogh L., Tomalia D. A., J. Am. Chem. Soc., **1998**, 120, 7355.

[77] Zhao M., Sun L., Crooks R. M., J. Am. Chem. Soc., **1998**, 120, 4877.

[78] Zhao,M., Crooks R. M., Angew. Chem., Int. Ed. Engl., **1999**, 38, 364.

[79] Hirai H., Nakao Y., Toshima N., J. Macromol. Sci., Chem. **1978**,
A12, 1117.

[80] Hirai H., Nakao Y., Toshima N., J. Macromol. Sci. Chem., **1979**, A13, 727.

[81] Hirai, H., J. Macromol. Sci. Chem., **1979**, A13, 633.

[82] Hirai H., Makromol. Chem. Suppl., **1985**, 14, 55.

[83] Hirai H., Nakao,Y., Toshima N., Chem. Lett., **1978**, 545.

[84] Smith T.W., US Patent 4252674.

[85] Tano T., Esumi K., Meguro K., J. Colloid Interface Sci., **1989**, 133, 530.

[86] Esumi K., Tano T., Meguro K., Langmuir, **1989**, 5, 268.

[87] Takahashi Y., Ito T., Sakai S., Ishii Y., Chem. Commun., 1**970**, 1065.

[88] Overbeek J.T.G., In Colloidal Dispersions, J.W. Goodwin (ed.), RSC, London, **1981.**

[89] Faraday M., Phil.Trans.Roy.Soc., **1857**, 147, 145.

[90] Klabunde K.J. (Ed), Nanoscale Materials in Chemistry, Wıley-Interscience Publishers, Newyork, **2001.**

[91] Aiken III J. D., Finke R.G., J.Molecular Catalyst, **1999,** 145, 1- 44.

[92] J. A. Widegren, J. D. Aiken, S. Özkar, R. G. Finke, Chem. Mater. 2001, **13**, 312.

[93] (a) Gaikwad A. V., Rothenberg G., Phys. Chem. Chem. Phys., **2006,** 8, 3669. (b) Creighton J. A., Eadon D. G., J. Chem. Soc. Faraday Trans. **1991,** 87, 3881.

[94] Tressaud A., Khairoun S., Touhara H., Watanabe N., Anorg. Allg. Chem., **1986,** 540, 291.

[95] Rioux R. M., Song H., Yang P., Somorjai G. A., Metal Nanoclusters in Catalysis and Materials Science: The Issue of Size Control, Ed. B. Corain, G.Schmid and N.Toshima, Elsevier, Netherlands, **2008**, Ch. 7.

[96] Palladium, JCPDS, 46-1043,**1969**.

[97] Kenneth Connors, Chemical Kinetics, 1990, VCH Publishers.

[98] Whitesides G. M., Hackett M., Brainard R. L., Lavalleye J. P., Sowinski A. F., Izumi A. N., Moore S. S., Brown D. W., Staudt E. M., Organometallics, **1985**, 4, 1819.

[99] Widegren J. A., Finke R. G., J. Mol. Catal. A: Chem., **2003**, 198, 317.

[100] Wagner C.D., Riggs W.M., Davis L.E., Moulder J.F., Muilenberg B.E. (Eds.), Handbook of X-Ray Photoelectron Spectroscopy, Perkin–Elmer Physical Electronics Division, Eden Prairie, p. 106,**1979**.

[101] McClune W.F., Powder Diffraction File Alphabetical Index, Inorganic Phase, JCPDS, Swarthmore, PA, **1980**.

APPENDIX A

Data for Activation Parameters of the Methanolysis of Ammonia-Borane Catalyzed by PVP Stabilized Palladium(0) and Ruthenium(0) Nanoclusters

The activation parameters of the methanolysis of ammonia-borane catalyzed by PVP stabilized palladium(0) and ruthenium(0) nanoclusters were determined by monitoring the hydrogen evaluation at different temperatures.

Table A.1 Volume of hydrogen versus time for the methanolysis of AB catalyzed by the PVP-stabilized palladium(0) nanoclusters starting with 200mM AB and 1.0mM Pd at different temperatures (15-35 $^{\circ}$C).

Time(Second)	**15 $^{\circ}$C**	**20 $^{\circ}$C**	**25 $^{\circ}$C**	**30 $^{\circ}$C**	**35 $^{\circ}$C**
0	0	0	0	0	0
30	2.4276	2.601	3.468	3.9882	4.234
60	5.8956	5.202	6.936	7.9764	8.468
90	9.3636	7.803	10.404	11.9646	12.702
120	12.8316	10.404	13.872	15.9528	16.936
150	14.5656	13.005	17.34	19.941	21.17
180	16.2996	15.606	20.808	23.9292	25.404
210	18.0336	18.207	24.276	27.9174	29.638
240	19.7676	20.808	27.744	31.9056	33.872
270	21.5016	23.409	31.212	35.8938	38.106
300	23.2356	26.01	34.68	39.882	42.34
330	24.9696	28.611	38.148	43.8702	46.574
360	26.7036	31.212	41.616	47.8584	50.808
390	28.4376	33.813	45.084	51.8466	55.042
420	30.1716	36.414	48.552	55.8348	59.276
450	31.9056	39.015	52.02	59.823	63.51
480	33.6396	41.616	55.488	63.8112	67.744
510	35.3736	44.217	58.956	67.7994	71.978
540	37.1076	46.818	62.424	71.7876	76.212

Table A.1 Continue

Time(Second)	**15°C**	**20°C**	**25°C**	**30°C**	**35°C**
570	38.8416	49.419	65.892	75.7758	80.446
600	40.5756	52.02	69.36	79.764	84.68
630	42.3096	54.621	72.828	83.7522	88.914
660	44.0436	57.222	76.296	87.7404	93.148
690	45.7776	59.823	79.764	91.7286	97.382
720	47.5116	62.424	83.232	95.7168	101.616
750	49.2456	65.025	86.7	99.705	105.85
780	50.9796	67.626	90.168	103.6932	110.084
810	52.7136	70.227	93.636	107.6814	114.318
840	54.4476	72.828	97.104	111.6696	118.552
870	56.1816	75.429	100.572	115.6578	122.786
900	57.9156	78.03	104.04	119.646	127.02
930	59.6496	80.631	107.508	123.6342	131.254
960	61.3836	83.232	110.976	127.6224	135.488
990	63.1176	85.833	114.444	131.6106	139.722
1020	64.8516	88.434	117.912	135.5988	143.956
1050	66.5856	91.035	121.38	139.587	148.223
1080	68.3196	93.636	124.848	143.5752	
1110	70.0536	96.237	128.316	147.5634	
1140	71.7876	98.838	131.784	148.223	
1170	73.5216	101.439	135.252		
1200	75.2556	104.04	138.72		
1230	76.9896	106.641	142.188		
1260	78.7236	109.242	145.656		
1290	80.4576	111.843	148.223		
1320	82.1916	114.444			
1350	83.9256	117.045			
1380	85.6596	119.646			
1410	87.3936	122.247			
1440	89.1276	124.848			
1470	90.8616	127.449			
1500	92.5956	130.05			
1530	94.3296	132.651			
1560	96.0636	135.252			
1590	97.7976	137.853			
1620	99.5316	140.454			
1650	101.2656	143.055			
1680	102.9996	145.656			
1710	104.7336	148.223			

Table A.1 Continue

Time(Second)	15°C	20°C	25°C	30°C	35°C
1740	106.4676				
1770	108.2016				
1800	109.9356				
1830	111.6696				
1860	113.4036				
1890	115.1376				
1920	116.8716				
1950	118.6056				
1980	120.3396				
2010	122.0736				
2040	123.8076				
2070	125.5416				
2100	127.2756				
2130	129.0096				
2160	130.7436				
2190	132.4776				
2220	134.2116				
2250	135.9456				
2280	137.6796				
2310	139.4136				
2340	141.1476				
2370	142.223				

Table A.2 Volume of hydrogen versus time for the methanolysis of AB catalyzed by the PVP-stabilized ruthenium(0) nanoclusters starting with 200mM AB and 1.5mM Ru at different temperatures (15-35 °C).

Time(Second)	15°C	20°C	25°C	30°C	35°C
0	0	0	0	0	0
15	4.2	5.7	7.6	9.6	11.4
30	6.1	9.5	11.4	15.7	19
45	7.2	13.3	15.2	23.2	26.6
60	8.3	15.2	19	28.5	34.2
75	9.4	19	22.8	34.2	41.8
90	10.5	22.8	28.5	39.9	49.4
105	11.6	24.7	32.3	45.6	57.8
120	12.7	26.6	36.1	51.3	65.6
135	13.8	30.4	41.8	57	72.2
150	14.9	32.3	45.6	62.7	79.2
165	16	36.1	49.4	68.4	87.4

Table A.2 Continue

Time(Second)	**15°C**	**20°C**	**25°C**	**30°C**	**35°C**
180	17.1	38	53.2	74.1	95
195	18.2	39.9	55.1	79.8	102.6
210	19.3	41.8	57	85.5	110.2
225	20.4	43.7	60.8	91.2	117.8
240	21.5	45.6	64.6	96.9	125.4
255	22.6	47.5	68.4	102.6	133
270	23.7	49.4	72.2	108.3	140.6
285	24.8	51.3	76	114	144.4
300	25.9	53.2	79.8	119.7	148.2
315	27	55.1	83.6	125.4	
330	28.1	57	87.4	131.1	
345	29.2	58.9	91.2	136.8	
360	30.3	60.8	95	142.5	
375	31.4	62.7	98.8	148.2	
390	32.5	64.6	102.6		
405	33.6	66.5	106.4		
420	34.7	68.4	110.2		
435	35.8	70.3	114		
450	36.9	72.2	117.8		
465	38	74.1	121.6		
480	39.1	76	125.4		
495	40.2	77.9	129.2		
510	41.3	79.8	133		
525	42.4	81.7	136.8		
540	43.5	83.6	140.6		
555	44.6	85.5	144.4		
570	45.7	87.4	148.2		
585	46.8	89.3			
600	47.9	91.2			
615	49	93.1			
630	50.1	95			
645	51.2	96.9			
660	52.3	98.8			
675	53.4	100.7			
690	54.5	102.6			
705	55.6	104.5			
720	56.7	106.4			
735	57.8	108.3			
750	58.9	110.2			

Table A.2 Continue

Time(Second)	**15°C**	**20°C**	**25°C**	**30°C**	**35°C**
765	60	112.1			
780	61.1	114			
795	62.2	115.9			
810	63.3	117.8			
825	64.4	119.7			
840	65.5	121.6			
855	66.6	123.5			
870	67.7	125.4			
885	68.8	127.3			
900	69.9	129.2			
915	71	131.1			
930	72.1	133			
945	73.2	134.9			
960	74.3	136.8			
975	75.4	138.7			
990	76.5	140.6			
1005	77.6	144.4			
1020	78.7	146.3			
1035	79.8	148.2			
1050	80.9				
1065	82				
1080	83.1				
1095	84.2				
1110	85.3				
1125	86.4				
1140	87.5				
1155	88.6				
1170	89.7				
1185	90.8				
1200	91.9				
1215	93				
1230	94.1				
1245	95.2				
1260	96.3				
1275	97.4				
1290	98.5				
1305	99.6				
1320	100.7				
1335	101.8				

Table A.2 Continue

Time(Second)	**15°C**	**20°C**	**25°C**	**30°C**	**35°C**
1350	102.9				
1365	104				
1380	105.1				
1395	106.2				
1410	107.3				
1425	108.4				
1440	109.5				
1455	110.6				
1470	111.7				
1485	112.8				
1500	113.9				
1515	115				
1530	116.1				
1545	117.2				
1560	118.3				
1575	119.4				
1590	120.5				
1605	121.6				
1620	122.7				
1635	123.8				
1650	124.9				
1665	126				
1680	127.1				
1695	128.2				
1710	129.3				
1725	130.4				
1740	131.5				
1755	132.6				
1770	133.7				
1785	134.8				
1800	135.9				
1815	137				
1830	138.1				
1845	139.2				
1860	140.3				
1875	141.4				
1890	143.5				
1905	147.6				